OXFORD

Human Molecular Genetics, 2015, Vol. 24, No. 24 7132–7150

doi: 10.1093/hmg/ddv413
Advance Access Publication Date: 3 October 2015
Original Article

ORIGINAL ARTICLE

APP overexpression in the absence of NPC1 exacerbates metabolism of amyloidogenic proteins of Alzheimer's disease

Mahua Maulik[1,2,3], Kyle Peake[3], JiYun Chung[1,4], Yanlin Wang[1,4], Jean E. Vance[3] and Satyabrata Kar[1,2,3,4,*]

[1]Centre for Prions and Protein Folding Diseases, [2]Centre for Neuroscience, [3]Department of Medicine, and [4]Department of Psychiatry, University of Alberta, Edmonton, AB T6G 2M8, Canada

*To whom correspondence should be addressed at: Centre for Prions and Protein Folding Diseases, Departments of Medicine (Neurology) and Psychiatry, University of Alberta, Edmonton, AB T6G 2M8, Canada. Tel: +1 7804929357; Fax: +1 7804929352; Email: skar@ualberta.ca

Abstract

Amyloid-β (Aβ) peptides originating from β-amyloid precursor protein (APP) are critical in Alzheimer's disease (AD). Cellular cholesterol levels/distribution can regulate production and clearance of Aβ peptides, *albeit* with contradictory outcomes. To better understand the relationship between cholesterol homeostasis and APP/Aβ metabolism, we have recently generated a bigenic ANPC mouse line overexpressing mutant human APP in the absence of Niemann-Pick type C-1 protein required for intracellular cholesterol transport. Using this unique bigenic ANPC mice and complementary stable N2a cells, we have examined the functional consequences of cellular cholesterol sequestration in the endosomal–lysosomal system, a major site of Aβ production, on APP/Aβ metabolism and its relation to neuronal viability. Levels of APP C-terminal fragments (α-CTF/β-CTF) and Aβ peptides, but not APP mRNA/protein or soluble APPα/APPβ, were increased in ANPC mouse brains and N2a-ANPC cells. These changes were accompanied by reduced clearance of peptides and an increased level/activity of γ-secretase, suggesting that accumulation of APP-CTFs is due to decreased turnover, whereas increased Aβ levels may result from a combination of increased production and decreased turnover. APP-CTFs and Aβ peptides were localized primarily in early-/late-endosomes and to some extent in lysosomes/autophagosomes. Cholesterol sequestration impaired endocytic-autophagic-lysosomal, but not proteasomal, clearance of APP-CTFs/Aβ peptides. Moreover, markers of oxidative stress were increased in vulnerable brain regions of ANPC mice and enhanced β-CTF/Aβ levels increased susceptibility of N2a-ANPC cells to H_2O_2-induced toxicity. Collectively, our results show that cellular cholesterol sequestration plays a key role in APP/Aβ metabolism and increasing neuronal vulnerability to oxidative stress in AD-related pathology.

Introduction

Alzheimer's disease (AD), the most common form of dementia affecting the elderly, is characterized by the presence of intracellular neurofibrillary tangles, extracellular β-amyloid (Aβ)-containing neuritic plaques and loss of neurons in selected brain regions (1,2). Assimilated evidence indicates that *in vivo* accumulation of Aβ may contribute to/trigger the loss of neurons and AD pathogenesis (3). These peptides are generated from the amyloid precursor protein (APP) which is processed by either non-amyloidogenic α-secretase or amyloidogenic β-secretase pathway (4). The α-secretase cleaves APP within the Aβ domain, yielding soluble APPα (sAPPα) and a C-terminal fragment (α-CTF) that is further processed by γ-secretase to generate $Aβ_{17–40}$/$Aβ_{17–42}$ fragments. Conversely, β-secretase cleaves APP to generate soluble APPβ (sAPPβ) and an Aβ-containing C-terminal fragment (β-CTF), which is processed via γ-secretase to yield full-length $Aβ_{1–40}$/$Aβ_{1–42}$.

Received: May 13, 2015. **Revised:** September 5, 2015. **Accepted:** September 28, 2015

While α-secretase processing occurs mostly in the secretory pathway, the endosomal–lysosomal (EL) system plays a critical role in the production of Aβ peptides (4).

Several studies show that cholesterol can influence APP processing and Aβ generation. For example, an increase in cellular cholesterol up-regulates, whereas a decrease down-regulates, Aβ generation in cultured neurons/cell lines (5,6). Moreover, a high-cholesterol diet has been reported to increase brain levels/deposition of Aβ, whereas a low-cholesterol diet can decrease the levels/deposition of Aβ in APP transgenic (Tg) mice (5,7). In contrast, some studies have reported that increased plasma cholesterol is associated with unchanged (8) or reduced (9) Aβ levels, while lowering plasma cholesterol either does not affect (10) or elevates (11,12) brain Aβ levels. Since plasma lipoproteins cannot cross the blood–brain barrier (13), it is important to determine how the cholesterol content of neurons influences the production/secretion of Aβ-related peptides.

Under normal conditions, cholesterol derived from astrocytes is taken up by neurons via receptor-mediated endocytosis and is delivered first to the EL system and then exported to other cellular compartments via a mechanism entailing the Niemann-Pick type C (NPC)-1 and -2 proteins (14–16). Although the overall cholesterol content isolated from Npc1-null mice is not higher than that of wild-type (WT) neurons, large amounts of cholesterol are sequestered in late-endosomes/lysosomes in cell bodies (17,18). Since the EL system is a major site of APP metabolism and exhibits marked changes in 'at risk' neurons prior to Aβ deposition in AD brains (4,19), it is important to determine how alterations in EL cholesterol levels can influence production and clearance of Aβ peptides. Interestingly, lack of NPC1 protein has been shown to cause AD-like phenotype including Aβ accumulation in human and mouse brains, while some recent studies have also reported altered expression of NPC1 in AD pathology (20–24). To better understand the functional link between NPC1 dysfunction, EL cholesterol sequestration and Aβ metabolism, we have recently developed a line of bigenic ANPC mice expressing familial AD mutant human APP on Npc1-null background. These ANPC mice display EL cholesterol sequestration and exhibit a phenotype more severe than either of the single mutants (APP-Tg or Npc1-null mice) including decreased life span, early cognitive and motor impairments, accelerated glial pathology, significant demyelination and exacerbated neurodegeneration (25). In the present study using this bigenic mice and a complementary stable neuronal N2a cell line, we show that cholesterol accretion within the EL system does not alter APP levels but increases APP-CTFs/Aβ levels, by increasing γ-secretase activity and impairing lysosomal clearance, rendering the cells vulnerable to oxidative stress in AD-related pathology.

Results

Influence of cholesterol sequestration on APP-CTFs and Aβ levels

Our recently generated bigenic ANPC mice that overexpress mutant human $APP_{KM670/671NL+V717F}$ in the absence of Npc1 protein exhibited decreased lifespan (i.e. ~11 weeks survival), early object memory and motor impairments, and exacerbated glial pathology (i.e. proliferation and activation of astrocytes and microglia and loss of oligodendrocytes) compared with APP-Tg and Npc1-null littermates. These ANPC mice sequester unesterified cholesterol in the EL system and display progressive loss of cerebellar Purkinje cells, whereas hippocampal neurons are relatively spared. These changes are accompanied by altered function of the EL system and increased phosphorylation and cleavage of tau protein in the cerebellum. In general, neuropathological abnormalities are more profound in the cerebellum than the hippocampus of ANPC mice (25). To determine if EL cholesterol sequestration triggered by the lack of Npc1 protein can alter levels and/or metabolism of human APP, we compared the expression profiles of APP mRNA and holoprotein in the vulnerable cerebellar region of ANPC ($APP^{+/0}Npc1^{-/-}$) mice to those from WT (WT: $APP^{0/0}Npc1^{+/+}$), APP-Tg ($APP^{+/0}Npc1^{+/+}$) and double heterozygous for mutant human APP and mouse Npc1 (Dhet: $APP^{+/0}Npc1^{+/-}$) littermates. The Npc1-null mice, on the other hand, do not express mutant human APP and thus have not been included for comparison. Our real-time qPCR analysis showed no significant difference in APP mRNA levels among APP-Tg, Dhet and ANPC littermates at 4- or 10-weeks of age, time points representing early and late stages of the pathogenesis in ANPC mice (Fig. 1A). Nor did immunoblotting of APP holoprotein with C-terminal APP antibodies reveal any differences among APP-Tg, Dhet and ANPC mice. As expected, the levels of APP were markedly higher in APP-Tg, Dhet and ANPC mice than in WT mice (Fig. 1B).

In the absence of differences in APP expression, we compared levels of the APP-cleaved products in brains of ANPC, APP-Tg and Dhet mice (Fig. 1C–F). The amount of α-CTF in the cerebellum of 10-week-old (but not 4-week-old) ANPC mice was approximately double that in APP-Tg and Dhet mice, whereas the β-CTF level was higher in both 4- and 10-week-old ANPC mice than in the other genotypes (Fig. 1C). However, the amounts of sAPPα and sAPPβ were not different in ANPC compared with APP-Tg and Dhet mice (Fig. 1D). In addition, the levels of human $Aβ_{1–40}$ and $Aβ_{1–42}$, as detected by enzyme-linked immunosorbent assay (ELISA), were significantly higher in the cerebellum of ANPC mice, compared with age-matched APP-Tg and Dhet mice (Fig. 1E and F); as expected, human $Aβ_{1–40}$/$Aβ_{1–42}$ were not detected in WT mice. Thus, cholesterol sequestration in the EL system of ANPC mouse cerebellum caused an accumulation of APP-CTFs and Aβ peptides in the absence of altered APP holoprotein levels.

To determine the mechanisms by which cholesterol sequestration in the EL system alters APP metabolism, we generated a complementary stable cell line by reducing Npc1 expression in mouse Neuro2a (N2a) cells that stably overexpressed the Swedish mutant human $APP_{KM670/671NL}$. The amounts of Npc1 mRNA and protein were ~90% lower in the *Npc1*-silenced cells (N2a-ANPC) than in control cells (N2a-APP) (Fig. 2A). Filipin staining of unesterified cholesterol revealed dense labeling in N2a-ANPC cells but only faint labeling in control N2a-APP cells, as expected (Fig. 2A). Consistent with the ANPC mice, depletion of Npc1 in N2a-ANPC cells increased the amounts of APP-CTFs (4- to 6-fold) and intracellular $Aβ_{1–40}$ (by ~50%) and $Aβ_{1–42}$ (by ~30%), but not full-length APP or intracellular sAPPα/sAPPβ (Fig. 2B–D). In addition, levels of Aβ peptides ($Aβ_{1–40}$/$Aβ_{1–42}$) (Fig. 2E) and sAPPα/sAPPβ (Fig. 2F) in the conditioned media of N2a-ANPC cells were not significantly different from those in N2a-APP cells, suggesting that cholesterol sequestration does not influence secretion of sAPP or Aβ peptides.

Cholesterol sequestration modulates APP processing

Since decreased levels/activity of γ-secretase might cause an accumulation of APP-CTFs, we first assessed the steady-state level of presenilin (PS1) and nicastrin components of this complex. In the cerebellum of ANPC mice, amounts of PS1 and nicastrin proteins were significantly higher than in WT, APP-Tg and Dhet mice (Fig. 3A and B). Moreover, levels of PS1 and mature nicastrin were

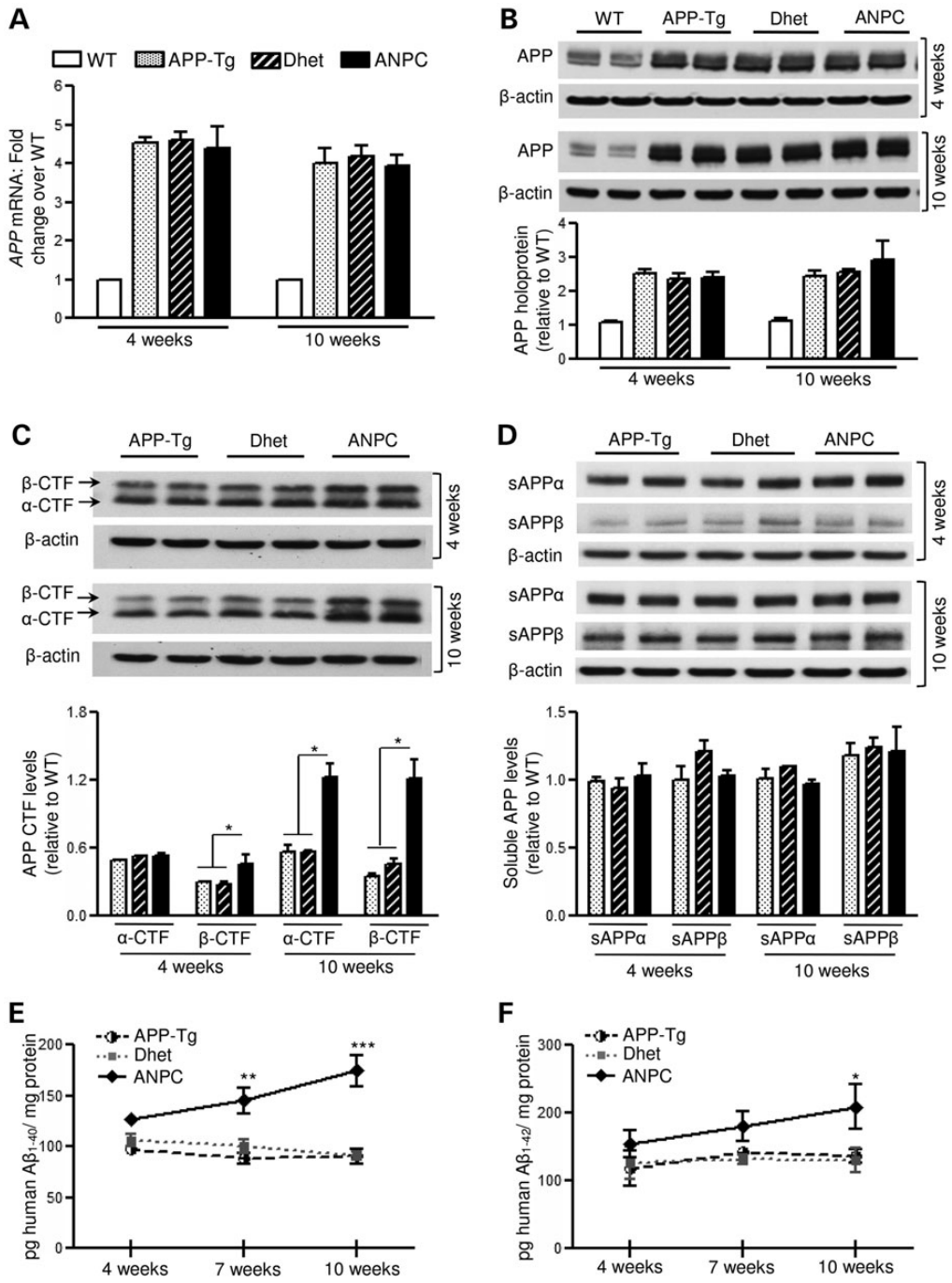

Figure 1. Increased levels of Aβ-related peptides in ANPC brains without any alteration in APP holoprotein or soluble APP fragments. (**A** and **B**) Real-time qPCR and immunoblotting analysis depicting APP mRNA (A) and holoprotein (~98 kDa, B) levels, respectively, in the cerebellum of WT, APP-Tg, Dhet and ANPC mice. (**C** and **D**) Immunoblots and corresponding histograms showing increased α- and β-CTFs (~10–12 kDa, C) but unaltered sAPPα and sAPPβ (D) fragments in the cerebellum of APP-Tg, Dhet and ANPC mice. (**E** and **F**) Age-dependent increase in human $A\beta_{1-40}$ (E) and $A\beta_{1-42}$ (F) levels in APP-Tg, Dhet and ANPC cerebellar homogenate, detected by ELISA. All blots were re-probed with anti-β-actin to monitor protein loading. Values are means ± SEM from 4 to 10 (i.e. ELISA, $n = 6–10$, qPCR and western blot, $n = 4$) mice/genotype/age. $^*P < 0.05$; $^{**}P < 0.01$; $^{***}P < 0.001$.

higher in N2a-ANPC than in N2a-APP cells (Fig. 3C). The activity of the γ-secretase complex was also markedly higher in the cerebellum of ANPC mice and in N2a-ANPC cells (Fig. 3D and E). The γ-secretase inhibitor N-[N-(3,5-Difluorophenacetyl)-L-alanyl]-S-phenylglycine t-butyl ester (DAPT) increased levels of APP-CTFs to a greater extent in N2a-ANPC cells than in N2a-APP cells (Fig. 3F) but strongly decreased $A\beta_{1–40}/A\beta_{1–42}$ in N2a-ANPC cells (Fig. 3G), suggesting that an enhanced level/activity of the γ-secretase complex possibly contributes to the increased processing of APP-CTFs in N2a-ANPC cells. To determine whether decreased turnover of peptides contributes to the enhanced levels of the peptides, cultured N2a-APP and N2a-ANPC cells were treated with cycloheximide to inhibit *de novo* synthesis of proteins including APP (26,27) and then

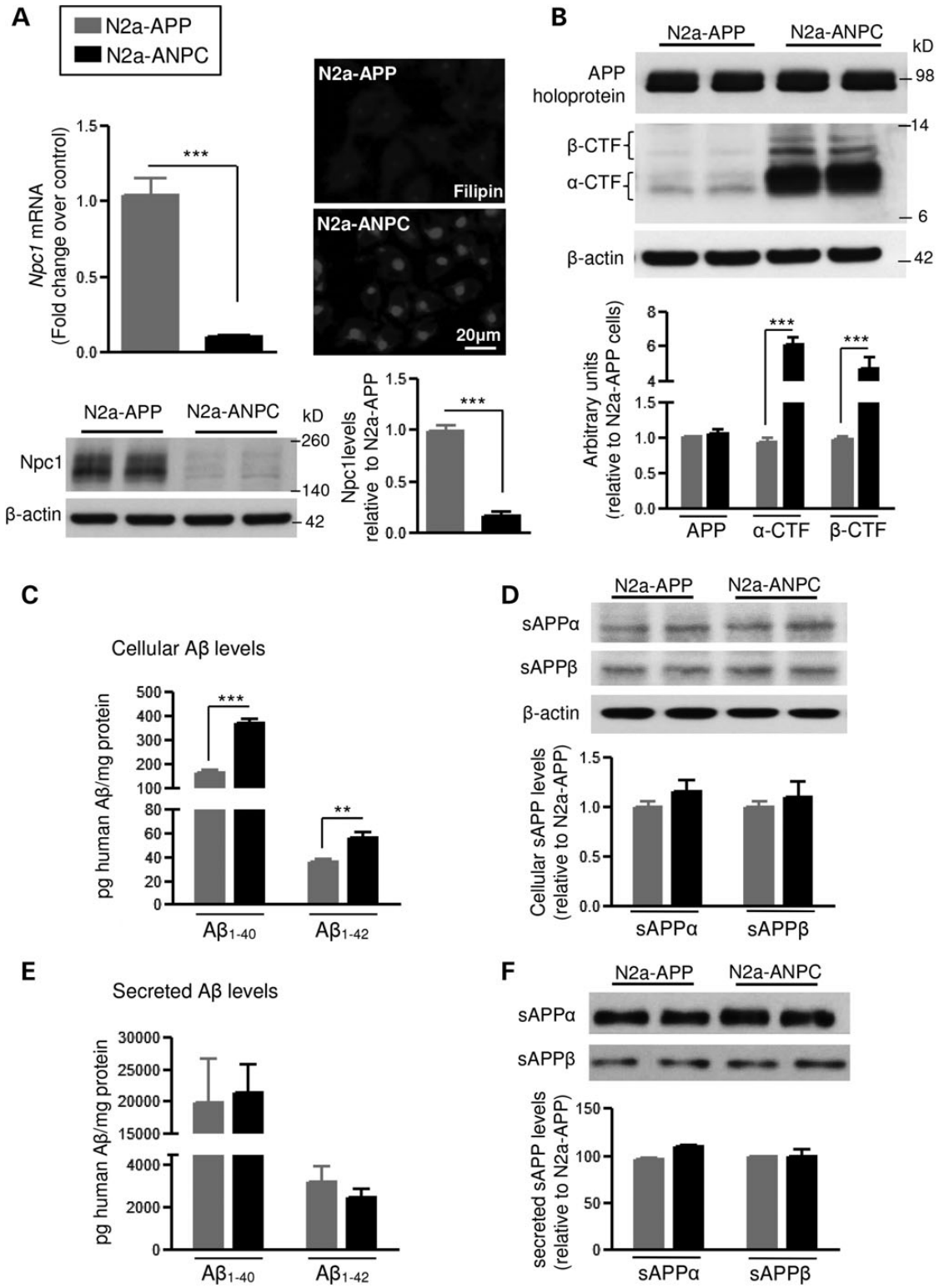

Figure 2. Consequence of Npc1 knock-down by Npc1-specific shRNA lentiviral infection in N2a cells overexpressing mutant human APP. (**A**) Histograms and representative immunoblot showing the efficiency of silencing *Npc1* mRNA and Npc1 protein in N2a-ANPC cells compared with N2a-APP cells transfected with scrambled shRNA. Fluorescence photomicrograph (on right) showing sequestration of unesterified cholesterol following reduction of Npc1 as observed by filipin labeling in N2a-ANPC and N2a-APP cells. (**B**) Representative immunoblots and histograms showing amounts of full-length APP, α-CTF and β-CTF in N2a-ANPC and N2a-APP cells. (**C** and **D**) Intracellular levels of human $A\beta_{1-40}$ and $A\beta_{1-42}$ (C, detected by ELISA) as well as soluble APP fragments (D, sAPPα and sAPPβ; detected by western blots) in N2a-ANPC cells and N2a-APP cells. (**E** and **F**) Quantification of human $A\beta_{1-40}$ and $A\beta_{1-42}$ (E, detected by ELISA) and soluble APP fragments (F, sAPPα and sAPPβ; detected by western blots) in conditioned media of N2a-APP and N2a-ANPC cells. All blots were reprobed with anti-β-actin antibody to monitor protein loading. Values represent means ± SEM of four independent experiments, each performed in duplicate. $^{**}P < 0.01$; $^{***}P < 0.001$.

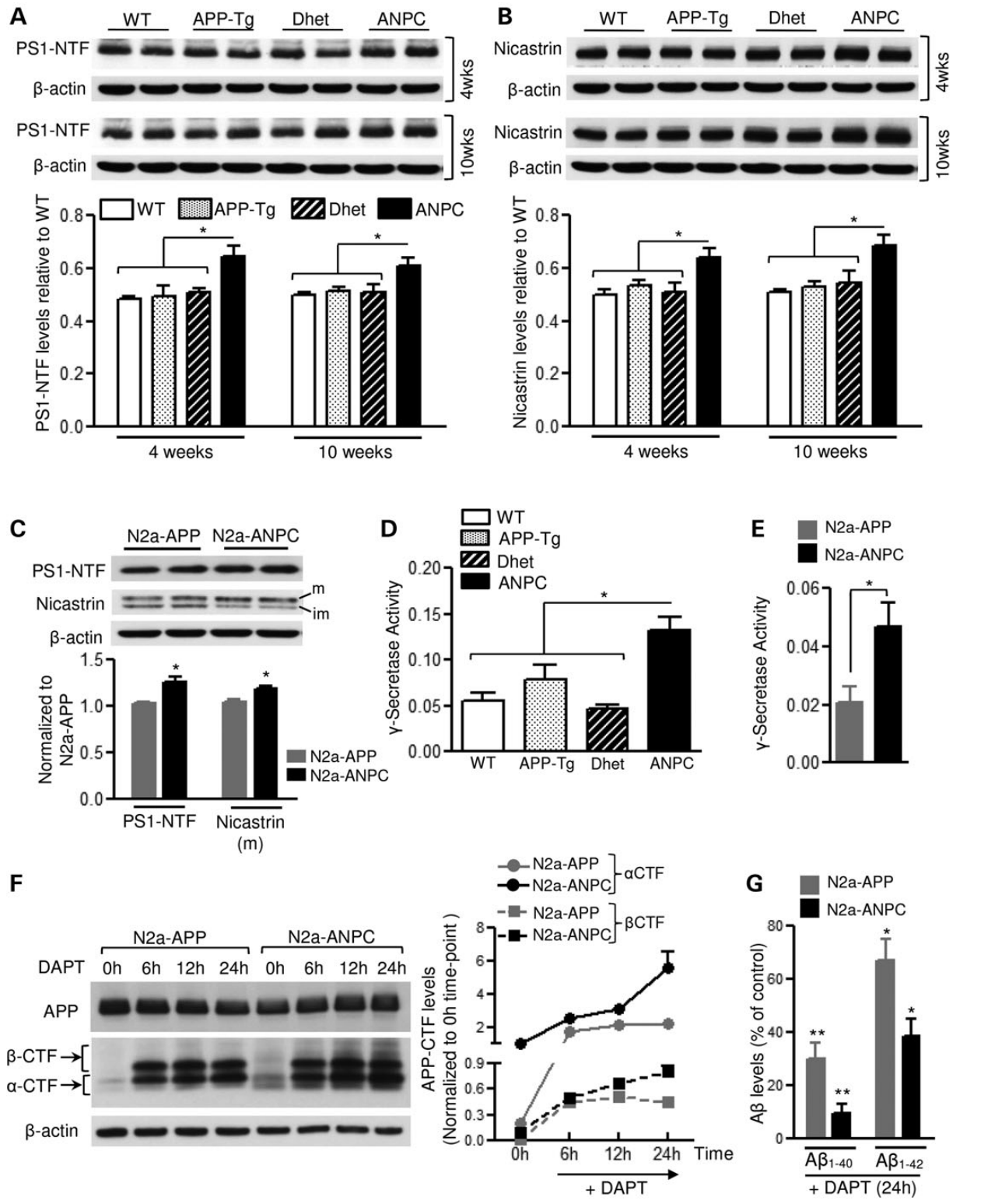

Figure 3. Effect of cholesterol sequestration on γ-secretase level and activity. (**A** and **B**) Immunoblots and histograms showing amounts of presenilin 1 (PS1-NTF ~27 kDa; A) and nicastrin (~110 kDa; B) in the cerebellum of 4- and 10-week-old WT, APP-Tg, Dhet and ANPC mice ($n = 4$ for 4 weeks/genotype, $n = 6$ for 10 weeks/genotype). (**C**) Immunoblots and histograms showing levels of PS1 and mature nicastrin in N2a-ANPC and N2a-APP cells ($n = 3$). (**D**) γ-Secretase activity in cerebellar homogenates of age-matched WT, APP-Tg, Dhet and ANPC mice ($n = 6$ per genotype). (**E**) γ-Secretase activity in N2a-ANPC and N2a-APP cells from five independent experiments. (**F** and **G**) Immunoblots and quantitation of amounts of APP-CTFs (α-CTF and β-CTF, F) and intracellular $A\beta_{1-40}$ as well as $A\beta_{1-42}$ (G) in N2a-ANPC and N2a-APP cells following treatment with 1 μM DAPT for 24 h ($n = 3$ independent experiments). All blots were re-probed with β-actin antibody to monitor protein loading. $^{*}P < 0.05$; $^{**}P < 0.01$.

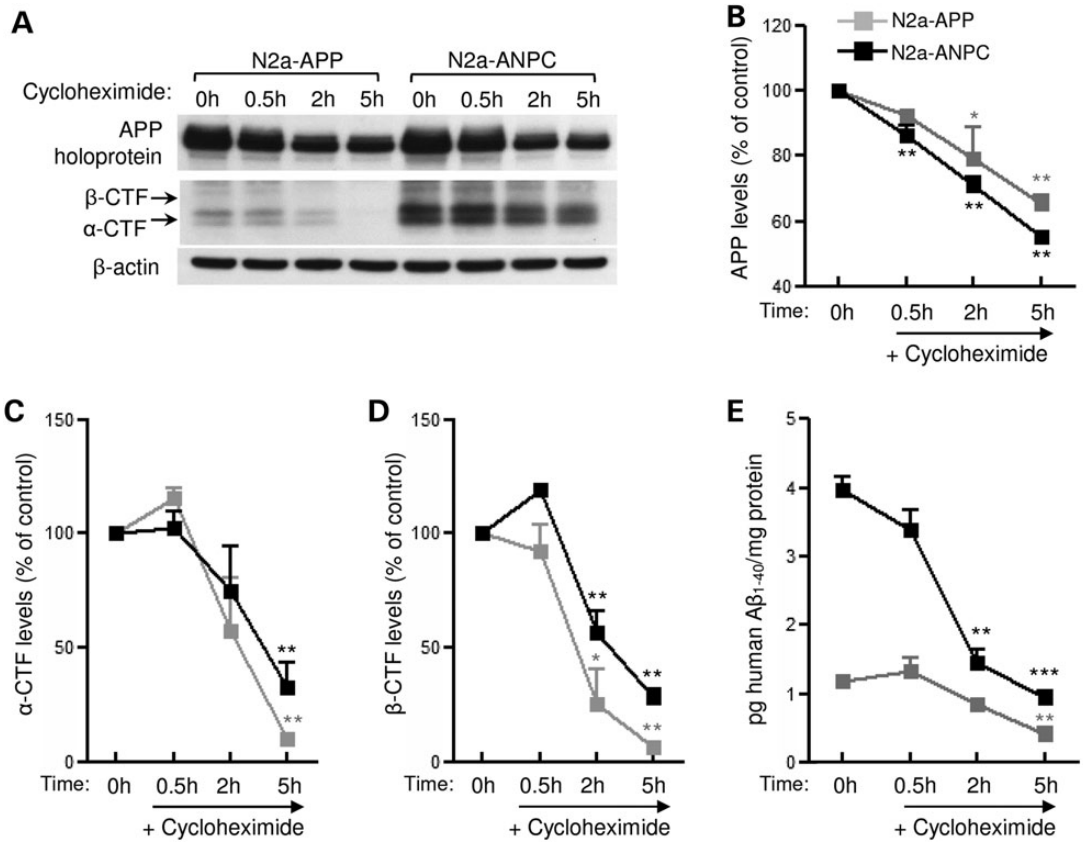

Figure 4. Effect of cholesterol sequestration on the clearance of APP, APP-CTFs and Aβ-related peptides. (**A–D**) Representative immunoblots of APP and APP-CTFs (A) and their respective quantifications (B–D) in cultured N2a-APP and N2a-ANPC cells following treatment with cycloheximide (30 μg/ml) for 0.5, 2 and 5 h. (**E**) Histogram showing human $A\beta_{1-40}$ levels (detected by ELISA) in cultured N2a-APP and N2a-ANPC cells following cycloheximide (30 μg/ml) treatment for 0.5, 2 and 5 h. All western blots were re-probed with anti-β-actin antibody to monitor protein loading. Data represent means ± SEM were from three independent culture experiments. $^{*}P < 0.05$, $^{**}P < 0.01$, $^{***}P < 0.001$.

steady-state levels of APP-CTFs and $A\beta_{1-40}$ were evaluated at different time points (Fig. 4A–E). Interestingly, our results clearly showed that levels of α-CTF/β-CTF (Fig. 4A, C and D) were markedly higher in cycloheximide-treated N2a-ANPC cells than in N2a-APP cells as a function of time suggesting a decreased rate of decay of the peptides following sequestration of cholesterol within EL system. The levels of $A\beta_{1-40}$ were also higher in N2a-ANPC cells compared with N2a-APP cells following treatment with cycloheximide (Fig. 4E). These data, together with unaltered levels of sAPPα/sAPPβ both in the cell lysates and in the conditioned media (Fig. 2D and F), indicate that the higher levels of APP-CTFs in N2a-ANPC cells and ANPC mouse brains are due to decreased turnover of APP-CTFs rather than decreased activity of γ-secretase, whereas the accumulation of Aβ might be the result of increased production and decreased turnover.

Influence of the proteasomal system on APP-CTF and Aβ levels

APP-CTFs, Aβ-related peptides and many core proteins involved in Aβ production, such as PS1, nicastrin and BACE1, are partly degraded by the proteasomal pathway (28,29). To determine whether the observed increase in APP-CTFs and Aβ was the consequence of impaired proteasomal activity, we measured chymotrypsin-like, trypsin-like and peptidyl-glutamyl peptide-hydrolyzing (PGPH)-like activities in the cerebellum of WT, APP-Tg, Dhet and ANPC mice (Supplementary Material, Fig. S1A). No significant alteration was evident in the activity of these enzymes in ANPC mice compared with the other genotypes. Additionally, levels of the catalytic β2-subunit of the proteasome system were equivalent in the cerebellum of WT, APP-Tg, Dhet and ANPC mice (Supplementary Material, Fig. S1B). Nor were proteasomal enzyme activities or catalytic β2-subunit levels, different between N2a-ANPC and N2a-APP cells (Supplementary Material, Fig. S1C and D). Thus, the accumulation of APP-CTFs and Aβ peptides are probably not due to decreased proteasomal activity. This conclusion is further supported by the finding that inhibition of proteasomal activity by MG132 increased the amounts of ubiquitinated proteins, APP-CTFs and Aβ peptides to similar levels in both N2a-APP and N2a-ANPC cells, independent of cholesterol sequestration (Supplementary Material, Fig. S1E–H).

Influence of the lysosomal system on APP-CTF and Aβ levels

The EL system mediates the degradation and recycling of unwanted cellular materials originating from two related pathways: endocytosis and autophagy (30,31). The endocytic pathway, comprising of early- and late-endosomes, serves as a site of origin/reservoir of APP-cleaved products including Aβ peptides, which are subsequently cleared, at least in part, by lysosomes (19,28). To determine if cholesterol sequestration triggered the accumulation of APP-CTFs and Aβ in the endocytic pathway, we assessed

the intracellular localization of these fragments under *in vivo* and *in vitro* conditions using confocal microscopy and endosomal and lysosomal markers. The sub-cellular localization of APP-CTFs was determined using an established monoclonal antibody Y188 developed against a synthetic peptide corresponding to the C-terminus of human APP (32,33). The characterization of staining recognized by the antibody was validated by double labeling of cultured N2a-ANPC cells which showed that Y188 immunoreactivity overlaps completely with another C-terminal APP antibody CTM1 but only partially with the N-terminal APP antibody 22C11 (see Supplementary Material, Fig. S2). Immunoreactive APP-CTFs and Aβ (detected by 4G8 antibody) exhibited diffuse, finely granular labeling in cerebellar neurons of WT, APP-Tg and Dhet mice, whereas in ANPC mice a more intense staining was evident as coarse granules. Double immunolabeling (Fig. 5A–P) indicated that in Purkinje cells of APP-Tg and ANPC mice, APP-CTFs and Aβ reside primarily in Rab5-positive early-endosomes (Fig. 5A–D), and to a lesser extent in Rab7-positive late-endosomes (Fig. 5E–H), but rarely in cathepsin D (CatD)- or Lamp1-positive lysosomes (Fig. 5I–L). The amounts of immunoreactive CTFs and Aβ peptides in early-endosomes were significantly higher in ANPC mice than in APP-Tg littermates (for CTFs: ANPC = 61.54 ± 3.932; APP-Tg = 43.33 ± 2.929; $P = 0.003$; for Aβ: ANPC = 44.17 ± 1.537; APP-Tg = 35.34 ± 1.591; $P = 0.004$). Filipin staining indicated that unesterified cholesterol colocalized mainly with CatD, not with APP-CTFs or Aβ peptides (Fig. 5M and N). However, in neurons of ANPC mice, a subset of CatD-containing vesicles that lacked filipin staining showed immunoreactivity for Aβ-related peptides (Fig. 5M and N). Moreover, Aβ immunoreactivity overlapped substantially with that of APP-CTFs in ANPC cerebellar neurons but less so in APP-Tg neurons (Fig. 5O and P).

In N2a-APP and N2a-ANPC cells, filipin-labeled cholesterol mostly associated with Lamp1-positive lysosomes (Fig. 5Q–T). Consistent with the *in vivo* data, immunoreactive APP-CTFs and Aβ peptides were more evident in a subset of early- and late-endosomes (not shown), as well as lysosomes, in N2a-ANPC than in N2a-APP cells (Fig. 5S and T). Since levels of APP-CTFs and Aβ in the ANPC cerebellum and N2a-ANPC cells were elevated compared with those in APP-Tg mice and N2a-APP cells, respectively, without any significant alteration of APP levels, we further conclude that the antigens recognized by 4G8 and Y188 antibodies are Aβ and APP-CTFs, rather than full-length APP.

Autophagy is considered to be the principal mechanism for degradation of long-lived normal and aggregated proteins as well as cellular organelles (34,35). Macroautophagy, usually referred to as autophagy, is the predominant form and involves formation of a double-membranous autophagosome that contains macromolecules and cell organelles and fuses with lysosomes for degradation of its contents. Interestingly, certain ubiquitinated proteins that are conjugated to the adaptor protein p62 are constitutively degraded by autophagy (36). Several studies indicate that altered functioning of the autophagic-lysosomal system plays a critical role in the generation and/or clearance of APP-CTFs and Aβ peptides (37,38). To determine if impairment of autophagy contributes to the accumulation of APP-CTFs and Aβ in ANPC mouse brains and N2a-ANPC cells, we assessed amounts of the autophagic marker LC3-II (Fig. 6). The steady-state level of LC3-II was higher in the cerebellum of ANPC mice than in WT, APP-Tg and Dhet mice (Fig. 6A). This increase was accompanied by enhanced LC3 immunoreactivity in cerebellar Purkinje cells suggesting accumulation of autophagic vesicles in ANPC brains (Fig. 6B). Double-labeling studies, however, revealed that only a subset of LC3-positive autophagic vesicles contained APP-CTFs and Aβ peptides, and that these vesicles were more abundant in ANPC mice than APP-Tg mice (Fig. 6B). Consistent with these *in vivo* data, the level and expression of LC3-II protein in N2a-ANPC cells was greater than in N2a-APP cells, and only a few LC3-positive autophagic vesicles exhibited immunoreactivity for APP-CTFs and Aβ peptides in N2a-ANPC cells (Fig. 6C).

In addition to increased amounts of LC3-II, the levels of p62 and ubiquitinated proteins in the cerebellum of 10-week-old ANPC mice were higher than in WT, APP-Tg and Dhet mice (Fig. 6D and E). Similarly, amounts of p62 (Fig. 6C) and ubiquitinated proteins (see Supplementary Material, Fig. S1E, Lanes 1 and 5) were also slightly higher in N2a-ANPC cells than in N2a-APP cells. Since proteasomal activity is not different between ANPC and APP-Tg mice (see Supplementary Material, Fig. S1A), it is likely that the increase in ubiquitinated proteins is the consequence of their reduced proteolysis by an abnormal autophagic-lysosomal system. This conclusion is supported by immunohistochemical data showing markedly increased expression of p62 and ubiquitin in LC3-positive autophagic vesicles in the Purkinje cells of ANPC, compared with APP-Tg mice (Fig. 6F).

Modulation of levels of APP-CTFs and Aβ peptides by the autophagic-lysosomal system

To validate the notion that the increased levels of APP-CTFs and Aβ peptides in ANPC mice and N2a-ANPC cells are due to impaired proteolysis via the endocytic/autophagic-lysosomal system, we used well-established pharmacological agents that are known to alter the function of the lysosomal network. In the presence of chloroquine, which prevents lysosomal clearance by neutralizing lysosomal pH (39), an increase in LC3-II was accompanied by markedly higher levels of APP-CTFs and Aβ peptides (Fig. 7A–C; Supplementary Material, Fig. S3A–C) in both N2a-APP and N2a-ANPC cells. As expected, since basal levels of APP-CTFs were already high in N2a-ANPC cells, the increase in APP-cleaved products, appeared earlier (by 2 h) in N2a-APP cells than in N2a-ANPC cells (by 5 h). Treatment of the cells with thapsigargin, which selectively blocks fusion of autophagosomes with lysosomes (40), also increased levels of LC3-II, APP-CTFs and Aβ peptides in both cell lines (Fig. 7D–F; Supplementary Material, Fig. S3D–F). In subsequent experiments, both N2a-APP and N2a-ANPC cells were treated with three distinct autophagy inhibitors, i.e. 3-methyladenine (3-MA), wortmannin and LY294002 (41–44). In the presence of 3-MA, a lower level of LC3-II was accompanied by increased levels of APP-CTFs and Aβ (Fig. 7G–I; Supplementary Material, Fig. S3G–I). More or less similar results for LC3-II and APP-CTFs were obtained with LY294002 (data not shown) and wortmannin (Supplementary Material, Fig. S4). Interestingly, dual treatment of cells with 3-MA and either chloroquine or thapsigargin produced an additive effect particularly on Aβ levels (Fig. 7J–O; Supplementary Material, Fig. S5A–F). These results, taken together, suggest that impairment of the trafficking/proteolysis, possibly due to neutralization of lysosomal pH caused by the sequestration of intracellular cholesterol, contributes to the accumulation of APP-CTFs and Aβ in N2a-ANPC cells and ANPC mouse cerebellum. This notion is reinforced by two distinct lines of experimental data. First, dual treatment with chloroquine and cycloheximide showed a lower rate of turnover for APP-CTFs in cultured N2a-ANPC cells than in N2a-APP cells (Fig. 8A–D). Second, we observed that the acidic milieu was less evident in N2a-ANPC cells than in N2a-APP cells according to staining with the ratiometric probe LysoSensor Yellow/Blue DND-160A, which produces yellow

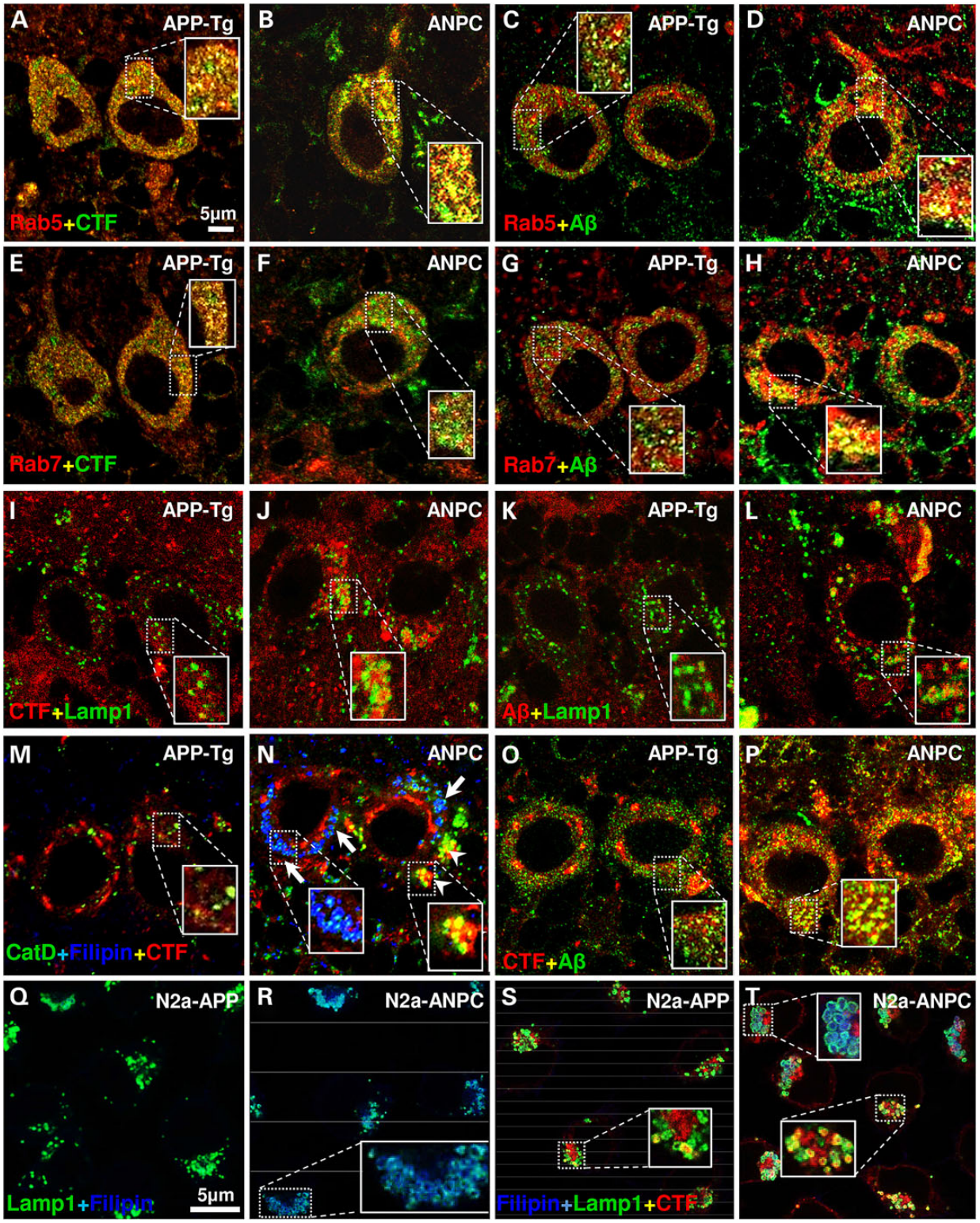

Figure 5. Effect of EL cholesterol accumulation on intracellular localization of Aβ-related peptides *in vivo* and *in vitro*. (**A–L**) Representative confocal images of cerebellar Purkinje neurons in APP-Tg and ANPC mice showing localization of immunoreactive APP-CTFs (clone Y188 or C1/6.1) and Aβ peptides (clone 4G8) in Rab5-positive early-endosomes (A–D), Rab7-positive late-endosomes (E–H) and Lamp1-positive lysosomes (I–L). (**M** and **N**) Triple labeling of Purkinje neurons in APP-Tg (M) and ANPC (N) mice showing that only a subset of CatD-positive vesicles that are free of filipin-positive unesterified cholesterol contain APP-CTFs in ANPC (N, arrowheads). Arrows indicate localization of unesterified cholesterol in CatD-positive vesicle. (**O** and **P**) Representative confocal images of Purkinje neurons showing co-localization of Aβ peptides with APP-CTFs in APP-Tg (O) and ANPC (P) mice. The immunoreactive profiles of various markers were verified in three mice/genotype. (**Q–T**) Confocal images of N2a-APP and N2a-ANPC cells showing localization of filipin in lamp1-positive lysosomes (Q and R) and that of APP-CTFs in a subset of Lamp1-positive lysosomes that do not contain unesterified cholesterol (S and T). The immunoreactive profiles of various markers in cultured cells were verified in three independent experiments. Identity of primary antibodies is indicated by respective font colors.

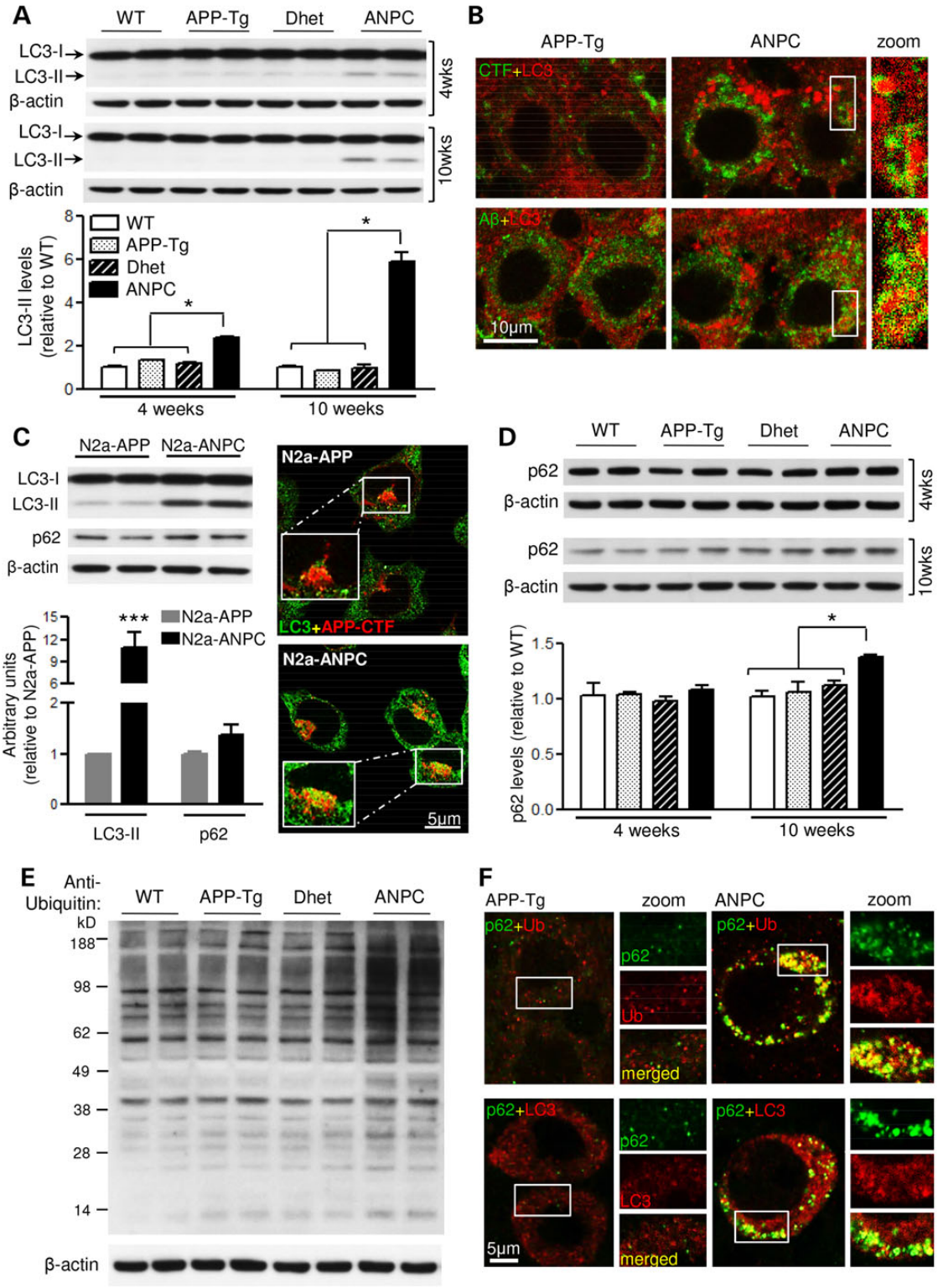

Figure 6. EL cholesterol impairs autophagic clearance *in vivo* and *in vitro*. (**A**) Immunoblots and histograms of LC3-II (~15 kDa) in the cerebellum of 4- and 10-week-old WT, APP-Tg, Dhet and ANPC mice ($n = 6$ mice/genotype/age). (**B**) Representative double immunostaining confocal images showing colocalization of LC3-labelled puncta with APP-CTFs and Aβ. Note the increased LC3 staining intensity in Purkinje cells of ANPC versus APP-Tg mice. The profile of immunostaining was verified in three mice/genotype. (**C**) Quantitative analysis of LC3-II and p62 (~62 kDa) levels along with representative confocal photomicrographs showing APP-CTFs in a subset of LC3-positive autophagic vesicles in N2a-APP/ANPC cells ($n = 3$). (**D**) Immunoblot quantitation of p62 levels in the cerebellum of 4- and 10-week-old WT, APP-Tg, Dhet and ANPC mice ($n = 6$ mice/genotype/age). (**E**) Representative immunoblot of ubiquitinated proteins in the cerebellum of 10-week-old WT, APP-Tg, Dhet and ANPC mice ($n = 4$ mice/genotype). (**F**) Representative confocal images showing co-localization of p62 with ubiquitin (upper panel) and LC3 (lower panel) in the cerebellar Purkinje neurons of ANPC and APP-Tg mice. The profile of immunostaining was verified in three mice/genotype. Identity of primary antibodies used is indicated by the respective font colors. All blots were re-probed with anti-β-actin. Data represent means ± SEM from 4 to 6 mice/genotype/age. $^{*}P < 0.05$; $^{***}P < 0.001$.

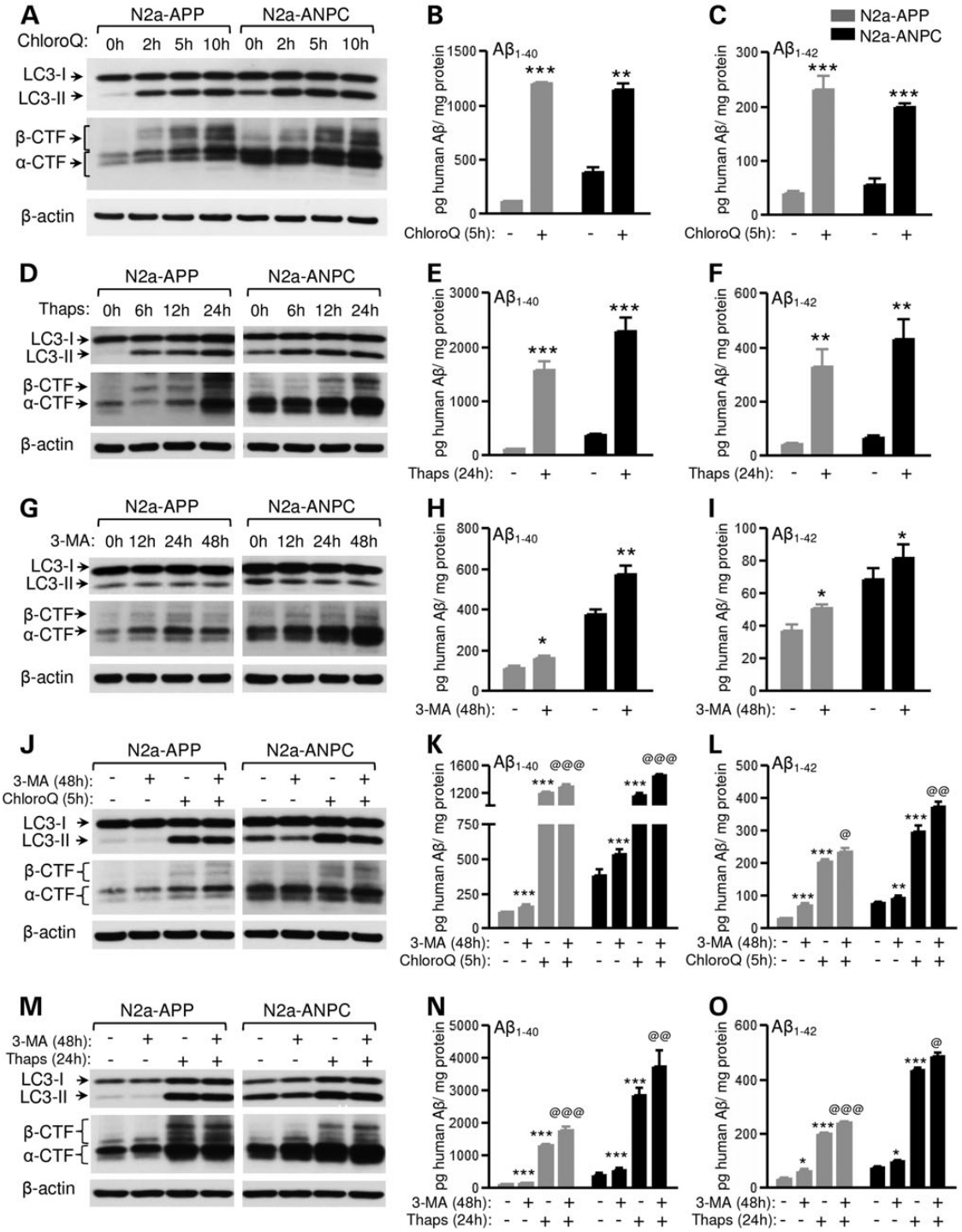

Figure 7. Pharmacologic inhibition of autophagic-lysosomal system triggers APP-CTFs and Aβ accumulation *in vitro*. (**A–C**) Representative immunoblots of LC3-II with APP-CTFs (A) and histograms showing human $A\beta_{1-40}/A\beta_{1-42}$ levels (B and C) in N2a-APP and N2a-ANPC cells following 50 μM chloroquine treatment. (**D–F**) Representative immunoblots of LC3-II with APP-CTFs (D) and histograms showing human $A\beta_{1-40}/A\beta_{1-42}$ levels (E and F) in N2a-APP and N2a-ANPC cells following 1 μM thapsigargin treatment. (**G–I**) Representative immunoblots of LC3-II with APP-CTFs (G) and histograms showing human $A\beta_{1-40}/A\beta_{1-42}$ levels (H and I) in N2a-APP and N2a-ANPC cells following 250 μM 3-MA treatment. (**J–L**) Representative immunoblots of LC3-II and APP-CTFs (J) as well as histograms showing human $A\beta_{1-40}/A\beta_{1-42}$ levels (K and L) in N2a-APP and N2a-ANPC cells following combined treatment with 3-MA (250 μM, 48 h) and chloroquine (50 μM, 5 h). (**M–O**) Representative immunoblots of LC3-II and APP-CTFs (M) as well as histograms showing human $A\beta_{1-0}/A\beta_{1-42}$ levels (N and O) in N2a-APP and N2a-ANPC cells following combined treatment with 3-MA (250 μM, 48 h) and thapsigargin (1 μM, 24 h). All blots were re-probed with anti-β-actin. '*' denotes significant difference between single treatment and no treatment; '@' indicates significant difference between combined treatment and single treatment. Data represent means ± SEM from three independent experiments for each treatment. $^{*}P < 0.05$; $^{**}P < 0.01$; $^{***}P < 0.001$.

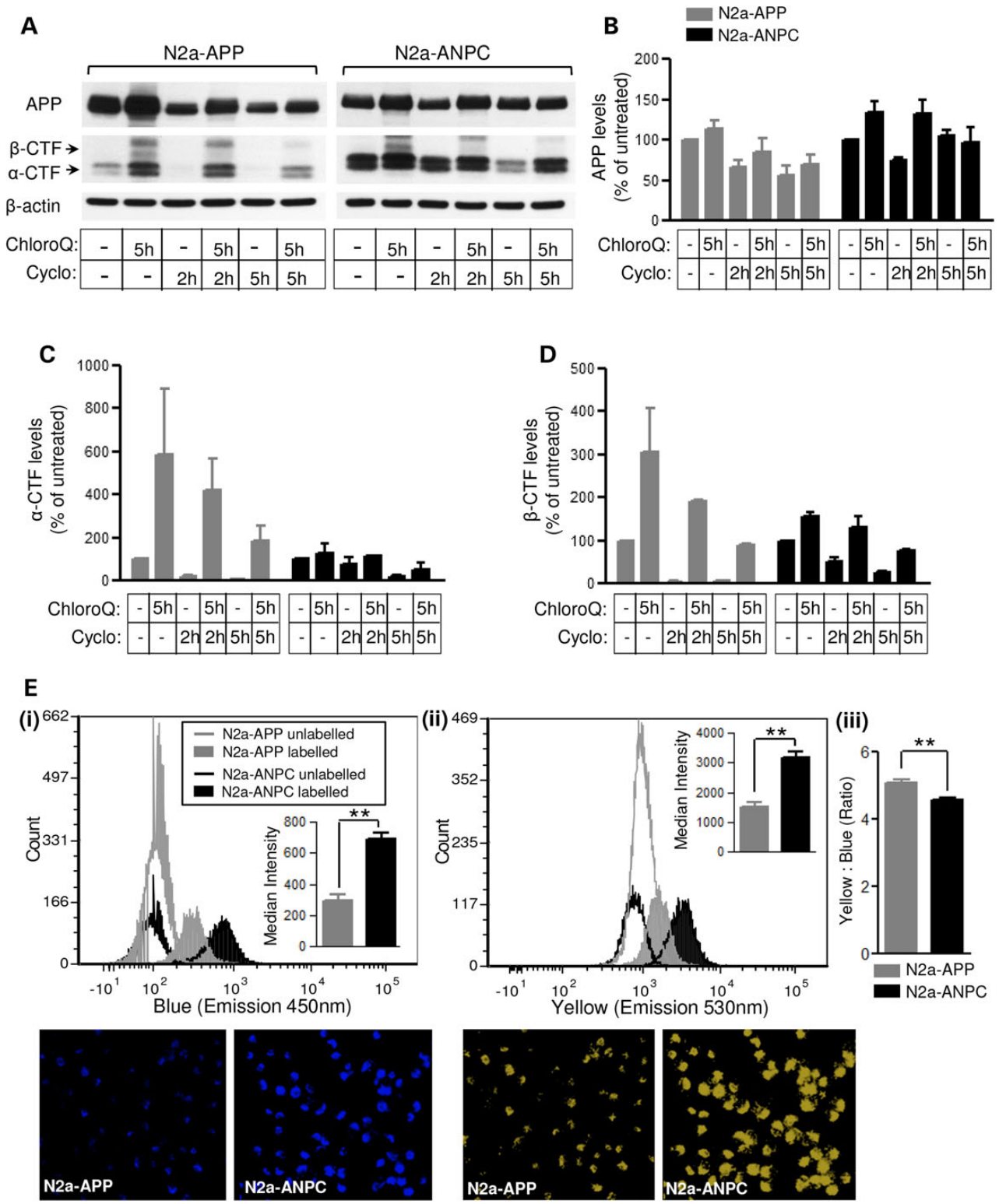

Figure 8. EL cholesterol sequestration impairs lysosomal clearance of APP-CTFs. (**A–C**) Representative immunoblots of APP and APP-CTFs (A) and their respective quantifications (B–**D**) in N2a-APP and N2a-ANPC cells following combined treatment with chloroquine (50 μM, 5 h) and cycloheximide (30 μg/ml, 2 and 5 h). (**E**) Flow cytometric analysis and microscopic images of cells stained with the ratiometric probe LysoSensor Yellow/Blue DND160 showing an overall increase in acidic yellow (ii) and less acidic blue (i) organelles in N2a-ANPC compared with N2a-APP cells. Note the significant decrease in yellow-to-blue intensity ratio (iii) in N2a-ANPC cells indicating reduction in the intracellular acidic milieu following EL cholesterol accumulation. Data represent means ± SEM from three independent experiments. $^{*}P < 0.05$; $^{**}P < 0.01$.

fluorescence in acidic organelles and blue fluorescence in less acidic organelles (Fig. 8E).

Influence of increased APP-CTFs and Aβ peptides on cell viability

Oxidative stress plays a role in neuronal degeneration in cholesterol-accumulating NPC disease, as well as in AD (45,46). Consistent with this idea, oxyblot experiments showed significantly more protein carbonyl groups, a marker of oxidative stress, in the cerebellum of 10-week-old, but not 4-week-old, ANPC mice compared with age-matched WT, APP-Tg and Dhet mice (Fig. 9A and B). Furthermore, in N2a-ANPC cells exposed to H_2O_2, levels of protein carbonylation were higher than in N2a-APP cells (Fig. 9C). In addition, N2a-ANPC cells were significantly more vulnerable to oxidative stress following H_2O_2 exposure than were N2a-APP cells (Fig. 9D). The toxicity induced by H_2O_2 was attenuated when the cells were pre-treated with inhibitors of either β-secretase [β-secretase inhibitor IV (BIV)] or γ-secretase (DAPT) (Fig. 9E and F). Since β-CTF and Aβ peptides can trigger cell death (47–49), it is likely that enhanced levels of these peptides in N2a-ANPC cells compared with N2a-APP cells may render them more vulnerable to H_2O_2-induced toxicity, though potential involvement of other molecules cannot be completely excluded. Interestingly, treatment of the cells with an inducer of autophagy, rapamycin, which triggers autophagic-flux and lysosomal biogenesis (50,51) also attenuated the H_2O_2-induced toxicity (Fig. 9G).

Discussion

Using bigenic ANPC mice and a neuronal cell line that stably overexpress mutant human APP in the absence of Npc1 protein, we show that sequestration of cholesterol within the EL system can render the cells vulnerable to oxidative injury by increasing the levels of APP-CTFs and Aβ peptides. While APP-CTFs levels are increased due to decreased turnover, enhanced levels of Aβ peptides are the result of increased production and decreased clearance mechanisms. Both APP-CTFs and Aβ peptides accumulate mostly in early- and late-endosomes, and partly in LC3-positive autophagosomes without any alterations in APP mRNA or protein levels. We also observed that cholesterol sequestration did not affect proteasomal activity but impaired the lysosomal clearance of APP-CTFs and Aβ peptides. Taken together, these results suggest that increased levels of β-CTF and Aβ peptides, as a consequence of cholesterol sequestration within EL system, can directly influence AD-related pathogenesis.

The critical factor by which cholesterol influences Aβ production might be not only the total cellular cholesterol level but also the compartmentalization of cholesterol within the cell (52). In neurons lacking Npc1 protein, the total cholesterol content is not increased, but cholesterol exit from late-endosomes/lysosomes is impaired (18,25). In this study, we show that cholesterol sequestration within the EL system does not influence APP mRNA or holoprotein levels either *in vitro* or *in vivo*. These observations are consistent with recent data showing that accumulation of cholesterol in neuronal cells, in response to the cholesterol transport inhibitor U18666A (20), or in brains of APP-Tg mice in which cholesterol synthesis was inhibited (53,54), did not affect APP levels. Nevertheless, we show that cholesterol accumulation within the EL system of ANPC mice and in N2a-ANPC cells significantly increased the amount of APP-CTFs (20,55). The levels of secreted sAPPα or sAPPβ, however, were not increased in either the cerebellum of ANPC mice or the cell lysates and media of N2a-ANPC cells. Since levels and activity of the γ-secretase complex are higher in ANPC mice and N2a-ANPC cells than in APP-Tg mice and N2a-APP cells, respectively, it is likely that the accumulation of APP-CTFs is a consequence of reduced proteolysis rather than increased production. This is validated by our cycloheximide experiments which showed a decreased turnover rate of APP-CTFs in N2a-ANPC cells compared with N2a-APP cells. In addition to APP-CTFs, levels of both $A\beta_{1-40}$ and $A\beta_{1-42}$ were increased in ANPC mice, as well N2a-ANPC cells, as previously reported in some cells/tissues with increased cholesterol content (20,22,56,57). The Aβ peptides that accumulate mostly in endosomes, and to a lesser extent in autophagic vesicles, in ANPC mice and cultured cells are derived, at least in part, from enhanced production, as indicated by the increased level/activity of the γ-secretase complex. Interestingly, however, in contrast to some reports (20,57), we observed that the secretory pool of Aβ was the same in N2a-ANPC and N2a-APP cells. Additionally, we showed that levels of $A\beta_{1-40}$ in cultured N2a-ANPC cells remained higher than in N2a-APP cells following cycloheximide treatment, thus suggesting that the intracellular accumulation of Aβ is also partially caused by decreased clearance of the peptide.

Many of the proteins involved in APP processing, like BACE1 and γ-secretase complex and a subset of the APP and Aβ-related peptides are partly degraded by proteasomes (29,58–60). Notwithstanding these data, we observed no differences either in the chymotrypsin-like, trypsin-like and PGPH-like activities or the catalytic β2 subunit of the ubiquitin–proteasomal system in the cerebellum of ANPC mice compared with other genotypes, or between N2a-ANPC and N2a-APP cells. Thus, we conclude that increased levels of APP-CTFs and Aβ observed in our studies are not caused by abnormalities in the ubiquitin–proteasome system. Interestingly, however, amounts of ubiquitinated proteins were found to be higher in the cerebellum of ANPC mice and N2a-ANPC cells compared with APP-Tg mice and N2a-APP cells, respectively. This likely reflects a decreased proteolysis of some p62-conjugated ubiquitinated proteins known to be degraded via the autophagic-lysosomal system (36). This conclusion is supported by the findings that levels of ubiquitinated proteins and p62 are higher in the cerebellum of ANPC mice compared with other genotypes, and that p62 and ubiquitin co-localize with LC3-positive autophagic vesicles in Purkinje cells of ANPC mice.

Lysosomes mediate the clearance of cellular substrates originating from endocytic and autophagic pathways (19,37). The significance of the autophagic pathway for APP metabolism, unlike endosomal system, remains somewhat controversial. Some studies conclude that inhibition of autophagy by 3-MA, wortmannin, LY294002 or by down-regulation of autophagy-related protein-5 decreases levels of APP-CTFs and Aβ (61–65). On the other hand, few studies indicate that induction of autophagy by beclin1 (66), or treatment with the autophagy enhancer rapamycin or SMER28, decreases levels of APP-CTFs and Aβ peptides (67,68). Alternatively, the autophagic pathway might not be directly involved in regulating APP metabolism (69). Our results clearly show that cholesterol sequestration within the EL system triggers APP-CTFs and Aβ accumulation in endosomal compartments and, to some extent, in LC3-positive autophagic vesicles, in the cerebellum of ANPC mice and N2a-ANPC cells. Interference with autophagy, by preventing formation of autophagosomes and/or the fusion of autophagosomes with lysosomes, significantly increased the levels of APP-CTFs and Aβ in N2a-APP and N2a-ANPC cells; in general, the changes were more pronounced in N2a-ANPC cells than in N2a-APP cells, likely due to higher basal levels of these proteins and/or their increased vulnerability to the inhibitors. These results, together with the observation

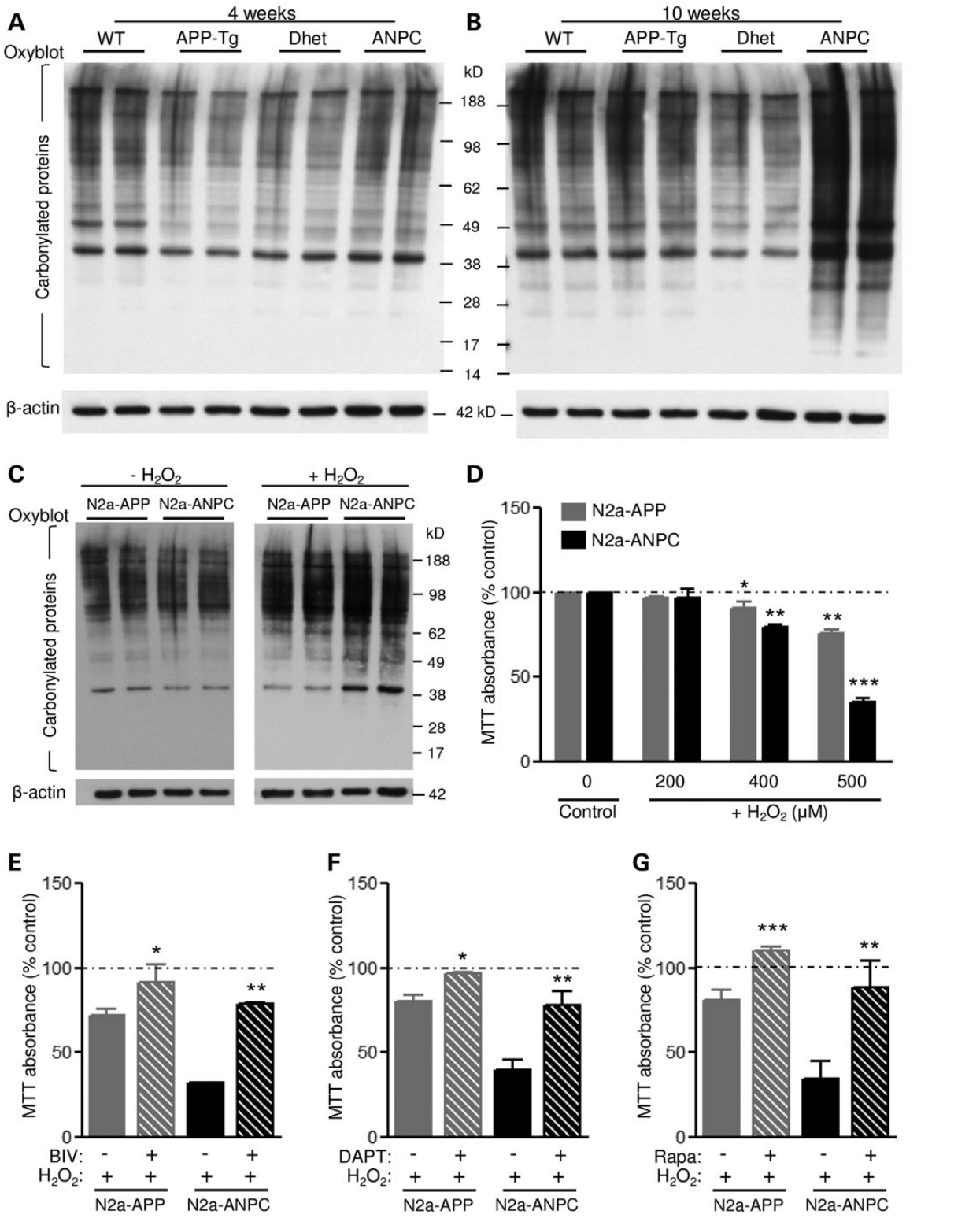

Figure 9. EL cholesterol sequestration increases oxidative stress and reduces cell viability. (**A–C**) Representative immunoblots of protein carbonyl levels, indicative of oxidative stress, in the cerebellum of 4- and 10-week-old WT, APP-Tg, Dhet and ANPC mice (A and B; $n = 4$ mice/genotype/age) and N2a-APP/ANPC cells (C) with and without exposure to 500 μM H_2O_2 for 3 h. (**D**) Histogram depicting MTT viability of N2a-APP and N2a-ANPC cells following 3 h treatment with H_2O_2 (0–500 μM). (**E–G**) Histograms showing reduced H_2O_2-induced toxicity of the cells upon 24 h pre-treatment with the β-secretase inhibitor BIV (10 μM, E), the γ-secretase inhibitor DAPT (1 μM, F) and the autophagy inducer rapamycin (10 μM, G). All blots were re-probed with anti-β-actin. Culture data represent means ± SEM from four independent experiments. $^*P < 0.05$; $^{**}P < 0.01$; $^{***}P < 0.001$.

that only a fraction of the LC3-positive vesicles contained APP-CTFs and Aβ in ANPC mouse brains, and in N2a-ANPC cells, clearly indicate that cholesterol sequestration within the EL system does not severely impair proteolysis of these molecules via autophagy. In contrast, direct hindrance of lysosomal activity/clearance with chloroquine markedly increased the levels of APP-CTFs and Aβ peptides in N2a-APP and N2a-ANPC cells. Since APP-CTFs and Aβ in ANPC mice and cultured cells accumulate primarily in EL compartments, rather than in autophagic vesicles, it implies that cholesterol sequestration profoundly affects the proteolysis of APP-CTFs/Aβ via the endosomal pathway than the autosomal pathway. This conclusion is substantiated by two findings (i) our results showing that chloroquine treatment reduced clearance of APP-CTFs more profoundly in N2a-ANPC cells than N2a-APP cells and (ii) the evidence that fusion of late-endosomes with lysosomes is impaired in cholesterol-accumulating Npc1-deficient cells (70,71). Nevertheless, future experiments are needed to define the relative significance of these degradative pathways in the clearance of APP-CTFs and Aβ from these cells.

Although the accumulation of β-CTF and Aβ-related peptides triggers neurodegeneration *in vitro* and *in vivo* (47–49), the significance of these peptides in neuronal loss consequent to EL cholesterol sequestration remains unclear. Oxidative damage, triggered by cholesterol accumulation, might play a role in the neuronal degeneration and the development of NPC as well as AD pathologies. Data in support of this concept are as follows: (i) degeneration of neurons by U18666A, a class-II amphiphile that triggers intracellular accumulation of cholesterol, is partly mediated by oxidative stress (72); (ii) synthesis of the antioxidant enzyme catalase or the antioxidant glutathione are diminished following cholesterol sequestration by Npc1 deficiency, whereas markers of oxidative stress are increased (46) and (iii) treatment of Npc1-deficient mice with the antioxidant curcumin and allopregnanolone increases lifespan and enhances viability of Purkinje cells (73,74). Our results are consistent with these data and show that N2a-ANPC cells are significantly more vulnerable than N2a-APP cells to H_2O_2-induced toxicity. Interestingly, treatment with inhibitors of β- and γ-secretase protected these cells from H_2O_2-induced toxicity, suggesting a direct role for accumulated β-CTF/Aβ peptides in oxidative cell death mechanism. This conjecture is reinforced by the finding that induction of autophagy and lysosomal biogenesis by rapamycin (50,51), which reduces levels of APP-CTFs and Aβ peptides (67,68), protected the cells against H_2O_2-induced toxicity. Thus, the accumulation of β-CTF and Aβ, in response to EL cholesterol sequestration, can render the cells vulnerable to oxidative cell death. In support of this idea, the affected cerebellar region of ANPC mice with enhanced levels of β-CTF and Aβ peptide shows a parallel increase in carbonyl protein levels—a well-established marker of oxidative injury. Under the circumstances, it is likely that enhanced levels of β-CTF and Aβ peptides may underlie the severe pathology and degeneration of neurons observed in the cerebellum of ANPC mice compared with other littermates (25). Additionally, given the evidence that Aβ peptide can induce cleavage/phosphorylation of tau protein (75,76) and activation of glial cells (77,78), it will be of interest to determine the potential role of the peptide in the development of glial pathology as well as abnormalities in tau protein observed in the cerebellum of ANPC mice (25).

In summary, using a new line of bigenic ANPC mice and N2a-ANPC cells stably expressing APP, we have shown that cholesterol accretion within the EL system does not alter the amount of APP but causes the accumulation of APP-CTFs and Aβ within endosomal and autophagic vesicles. The increase in these peptides is a consequence of increased production and/or decreased turnover via the lysosomal pathway. Additionally, the accumulation of both β-CTFs and Aβ increases the vulnerability of the cells to oxidative injury which may underlie the loss of neurons in AD as well as NPC disease. Overall, our results provide novel insights into the functional relationship between EL cholesterol accretion and APP metabolism and their significance in AD-related pathogenesis.

Materials and Methods

Reagents

NuPAGE 4–12% Bis-Tris gels, Alexa Fluor 488/594-conjugated secondary antibodies, ProLong Gold anti-fade reagent, DNase I, oligo $(dT)_{12–18}$ primers, SuperScript™ II Reverse Transcriptase and ELISA kits for the detection of human $Aβ_{1–40}$ and $Aβ_{1–42}$ were purchased from Life Technologies. The DNA and RNA isolation kits were from Qiagen, while iQ™ SybrGreen supermix was from Bio-Rad, Inc. All genotyping and real-time PCR primers were from Integrated DNA Technologies. Filipin, chloroquine, 3-MA, wortmannin, LY294002, cycloheximide, thapsigargin and γ-secretase inhibitors (DAPT and L-685,458) were obtained from Sigma-Aldrich. The bicinchoninic acid protein assay kit and enhanced chemiluminescence kit were from ThermoFisher Scientific. Vivaspin filtration columns were from GE Healthcare and Oxyblot™ protein oxidation kit was from EMD Millipore. The β-secretase inhibitor BIV, proteasomal inhibitor MG132 and fluorogenic γ-secretase substrate were from Calbiochem, while rapamycin was from LC laboratories. Proteasomal fluorogenic substrates were from Enzo Life Sciences or Calbiochem. Sources of all the primary antibodies are listed in Table 1. Horseradish peroxidase-conjugated secondary antibodies were purchased from Santa Cruz Biotechnology. All other chemicals were from Sigma-Aldrich or ThermoFisher Scientific.

Mice

Mutant human $APP_{KM670/671NL+V717F}$ Tg mice (TgCRND8) maintained on a C3H/C57BL6 background (79) were crossed with heterozygous Npc1-deficient mice on a BALB/c background to generate bigenic ANPC, Dhet, APP-Tg and WT mice on a C3H/C57BL6/BALB/c background (25). All animals were maintained on a 12 h light/dark cycle and bred and housed with access to food and water *ad libitum*. Maintenance of the breeding colony and experiments involving animals complied with Institutional and Canadian Council of Animal Care guidelines. All mice were genotyped twice by PCR analysis of tail DNA: initially at weaning (21 days) and at euthanisation.

Cell culture, development of stable cell lines and drug treatments

Mouse Neuro2a (N2a) neuroblastoma cells stably overexpressing the human Swedish mutant (K670N, M671L) APP (N2aAPPsw, clone Swe.10) were the generous gift of Dr G. Thinakaran (The University of Chicago, IL, USA) and maintained in N2a growth medium as described earlier (80). The amount of Npc1 protein was reduced in N2aAPPsw cells (referred as N2a-ANPC) by mRNA silencing with lentiviruses expressing *Npc1* shRNA and subjected to puromycin selection according to manufacturer's instructions (Santa Cruz Biotechnology). The controls, N2aAPPsw cells, were transduced with lentiviral shRNA encoding a scrambled sequence (referred as N2a-APP). Cultured N2a-APP and N2a-ANPC cells were treated with H_2O_2 (0–500 μm), MG132

Table 1. Primary antibodies used

Antibody	Type	IF dilution	WB dilution	Source
APP (clone Y188)	Monoclonal	1:250	1:5000	Abcam Inc.
APP (clone C1/6.1)	Monoclonal	1:1000	n/a	Covance Corp.
APP (clone 22C11)	Monoclonal	1:2000	n/a	EMD Millipore Co.
APP (clone CTM1)	Polyclonal	1:2000	n/a	Kind gift from Dr G. Thinakaran, University of Chicago, USA
Cathepsin D (CatD)	Polyclonal	1:200	n/a	Santa Cruz Biotechnology, Inc.
Lamp1 (clone ID4B)	Monoclonal	1:500	n/a	Developmental studies, Hybridoma Bank, Univ. of Iowa, USA
LC3	Polyclonal	1:1000	1:1000	MBL International Corp.
Nicastrin	Polyclonal	n/a	1:500	Santa Cruz Biotechnology, Inc.
p62 (sequestosome-1)	Monoclonal	1:100	1:1000	EMD Millipore Co.
Presenilin1-NTF (PS1-NTF)	Polyclonal	n/a	1:3000	Kind gift from Dr G. Thinakaran, University of Chicago, USA
Proteasome subunit beta type 2 (β2)	Monoclonal	n/a	1:1000	Abcam Inc.
Rab5	Polyclonal	1:200	n/a	Abcam Inc.
Rab7	Polyclonal	1:500	n/a	Sigma-Aldrich, Inc.
sAPPα (2B3)	Monoclonal	n/a	1:1000	IBL Co., Ltd
sAPPβ-sw (6A1)	Monoclonal	n/a	1:3000	IBL Co., Ltd
Ubiquitin	Polyclonal	1:250	1:200	Santa Cruz Biotechnology, Inc.
β-Actin	Monoclonal	n/a	1:5000	Sigma-Aldrich, Inc.
β-Amyloid, 1–16 (6E10)	Monoclonal	1:1000	1:3000	Covance Corp.
β-Amyloid, 17–24 (4G8)	Monoclonal	1:1000	n/a	Covance Corp.

IF, immunofluorescence; WB, western blotting; n/a, not used in that application.

(10 μM), chloroquine (50 μM), 3-MA (250 μM), wortmannin (0.1 μM), LY294002 (10 μM), cycloheximide (30 μg/ml), rapamycin (10 μM), thapsigargin (0.1 μM), γ-secretase inhibitor DAPT (1 μM) or BACE1 inhibitor BIV (10 μM) in the growth medium for indicated durations. The concentration of BIV and DAPT used in the study did not compromise viability of either N2a-APP or N2a-ANPC cells. Cells were harvested and either used immediately or stored at −80°C until further processing.

Real-time PCR

RNA from mouse cerebellar tissues (WT, APP-Tg, Dhet and ANPC mice), and cultured N2a-APP and N2a-ANPC cells, was isolated using the RNeasy lipid tissue and RNeasy RNA extraction kit, respectively. RNA (2 μg) was treated with DNaseI and reverse transcribed using oligo(dT)$_{12–18}$ primers and SuperScript™ II Reverse Trancriptase. Quantitative real-time PCR was performed with iQ™ SybrGreen supermix in a MyiQ™ Cycler with iQ5 real-time detection system (Bio-Rad Laboratories). Primer sequences were: *APP* (forward, 5′-GCCAAAGAGACATGCAGTGA-3′ and reverse, 5′-CCAG ACATCCGAGTCATCCT-3′, spanning regions from both human and mouse APP), *Npc1* (forward, 5′-CACCAATCCTGTAGAGCTCTG-3′ and reverse, 5′-GGAAGGTGATCACAAGCGCGG-3′) and *β-actin* (forward, 5′-AGCCATGTACGTAGCCATCC-3′ and reverse, 5′-CTCTCA GCTGTGGTGGTGAA-3′). Each sample was assayed in duplicate and mRNA normalized to *β-actin* mRNA.

Western blotting

Western blotting was performed as described earlier (25) on mouse brain cerebellar homogenates (4–6 mice/genotype/age), as well as cultured cells using anti-APP, anti-Aβ, anti-sAPPα, anti-sAPPβ, anti-nicastrin, anti-PS1, anti-p62, anti-LC3, anti-ubiquitin or anti-proteasomal β2 subunit antisera at dilutions listed in Table 1. All blots were re-probed with anti-β-actin antibodies and quantified using a MCID image analyzer (Imaging Research, Inc.).

Immunostaining and confocal microscopy

Mice of the different genotypes (WT, APP-Tg, Dhet and ANPC; 3–5 mice/genotype) at 7–8 weeks of age were perfusion fixed with 4% paraformaldehyde and their cerebellar cryostat sections (20 μm) were processed for immunofluorescence labeling (25,55). With regard to cultures, cells grown on glass coverslips were fixed with 4% paraformaldehyde and processed for immunocytochemistry. For sub-cellular localization of antigens, fixed brain sections/cells were incubated overnight at 4°C with anti-APP or anti-Aβ combined with anti-Rab5, anti-Rab7, anti-CatD, anti-Lamp1, anti-p62, anti-ubiquitin or anti-LC3 antibodies (dilutions in Table 1) and then processed as described earlier (25,55). For visualization of unesterified cholesterol, immunolabeled sections/cells were incubated with 25 μg/ml filipin in the dark. Immunostained sections/cells were visualized and imaged using a Zeiss multiphoton confocal laser scanning microscope (LSM510, Carl Zeiss, Inc.) equipped with a 63× Plan-apochromatic oil-immersion lens. For quantification of the extent of colocalization, images were deconvoluted using Huygens Elements-XI software (Scientific Volume Imaging) and quantified using the Imaris 7.5.1 software (Bitplane AG).

Flow cytometry

N2a-APP and N2a-ANPC cells were incubated with LysoSensor yellow/Blue DND-160 (1 μM) for 30 min in N2a growth medium, washed and analyzed using LSR-Fortessa Flow Cytometer (BD Biosciences). The two detectors had 450/50 nm and 530/30 nm filters with excitation of 355 nm (20 mW UV laser). Data were analyzed using FCS Express 4 Flow Cytometry software (De Novo Software).

In vitro γ-secretase activity assays

γ-Secretase activity in the cerebellum of 10-week-old mice (WT, APP-Tg, Dhet and ANPC; 3–5 mice/genotype), and in cultured

N2a-APP and N2a-ANPC cells, was measured as described previously (81). Enzymatic activity was determined by incubating a parallel set of samples with 100 μM γ-secretase inhibitor L-658,458. All samples were assayed in duplicate, and results were from five independent experiments.

ELISA for $A\beta_{1-40}$ and $A\beta_{1-42}$

Human $A\beta_{1-40}$ and $A\beta_{1-42}$ levels in the cerebellum of 4-, 7- and 10-week-old ANPC, APP-Tg, Dhet and WT mice (4–6 mice/genotype/age), and cultured N2a-APP and N2a-ANPC cells were measured using commercially available ELISA kits as described earlier (79). For Aβ in conditioned media, cells were incubated in 6 ml of serum-free Opti-MEM I for 3 h and subsequently human $A\beta_{1-40}$/$A\beta_{1-42}$ levels were measured by ELISA. All samples were assayed in duplicate, and each experiment was repeated three times.

Detection of proteasomal activities

Brain cerebellar tissue from 4- and 10-week-old WT, APP-Tg, Dhet and ANPC mice, as well as cultured N2a-APP and N2a-ANPC cells, was homogenized, centrifuged and proteasome peptidase activities measured in supernatants as described earlier (82). Fluorogenic substrates (Suc-LLVY-AMC, Boc-LRR-AMC and Z-LLE-AMC) were used to estimate chymotryptic-like, tryptic-like and PGPH-like proteasomal activities, respectively. All samples were assayed in triplicate, and proteasome activity was expressed as fluorescence units/μg protein/min after subtraction of the values obtained in the presence of 1 μM MG132, a general proteasomal inhibitor.

Detection of oxidative stress

Cerebellar tissues from 4- and 10-week-old WT, APP-Tg, Dhet and ANPC mice, and cultured N2a-APP and N2a-ANPC cells, were assayed for protein carbonyl content using the Oxyblot™ protein oxidation kit following manufacturer's protocol. All blots were re-probed with anti-β-actin to monitor protein loading.

Viability of cultured cells

Viability of N2a-APP and N2a-ANPC cells treated with H_2O_2 in the presence or absence of various drugs was determined using the colorimetric MTT assay (83). Each experiment was performed in triplicate and repeated three to four times.

Statistical analysis

Data are expressed as means ± SEM. Statistical significance of differences was determined by one-way ANOVA followed by Newman–Keuls post-hoc analysis for multiple comparisons or unpaired two-tailed Student's *t*-test for single comparison with a significance threshold of $P < 0.05$. All analyses were performed using GraphPad Prism Software.

Supplementary Material

Supplementary Material is available at *HMG* online.

Acknowledgements

We thank Dr G. Thinakaran (The University of Chicago, IL, USA) for his generous gift of PS1-NTF and CTM1 antibodies and N2aAPPsw (clone Swe.10) stable cell lines. The Lamp1 monoclonal antibody developed by Dr J.T. August was obtained from the Developmental Studies Hybridoma Bank, The University of Iowa, Iowa City, IA 52242, USA. We also thank Dr X. Sun and G. Barron (Cross Cancer Institute Cell Imaging Facility, Univ. of Alberta) for assistance with confocal microscopy, and Dr A. Holme and D. Kratochwil-Otto (Flow Cytometry Core Facility, Univ. of Alberta) for flow cytometry experiments.

Conflict of Interest statement. The authors have no conflict of interest.

Funding

This work was supported by grants from Canadian Institutes of Health Research (MOP-123258 to S.K.), the University of Alberta Hospital Foundation (RES0021060 to S.K.) and the Ara Parseghian Medical Research Foundation (J.E.V.). M.M. is a recipient of President's International Doctoral Award from the University of Alberta and a studentship award from Alberta Innovates Health Solutions (AIHS). K.P. is a recipient of studentship awards from the AIHS and the Natural Sciences and Engineering Research Council of Canada. Y.W. is a recipient of studentship awards from Alzheimer Society of Canada and AIHS.

References

1. Selkoe, D.J. (2011) Alzheimer's disease. *Cold Spring Harb. Perspect. Biol.*, **3**, doi: 10.1101/cshperspect.a004457.
2. Karch, C.M., Cruchaga, C. and Goate, A.M. (2014) Alzheimer's disease genetics: from the bench to the clinic. *Neuron*, **83**, 11–26.
3. Hardy, J., Bogdanovic, N., Winblad, B., Portelius, E., Andreasen, N., Cedazo-Minguez, A. and Zetterberg, H. (2014) Pathways to Alzheimer's disease. *J. Intern. Med.*, **275**, 296–303.
4. Haass, C., Kaether, C., Thinakaran, G. and Sisodia, S. (2012) Trafficking and proteolytic processing of APP. *Cold Spring Harb. Perspect. Med.*, **2**, a006270.
5. Fassbender, K., Simons, M., Bergmann, C., Stroick, M., Lutjohann, D., Keller, P., Runz, H., Kuhl, S., Bertsch, T., von Bergmann, K. *et al.* (2001) Simvastatin strongly reduces levels of Alzheimer's disease beta-amyloid peptides Abeta 42 and Abeta 40 in vitro and in vivo. *Proc. Natl. Acad. Sci. USA*, **98**, 5856–5861.
6. Simons, M., Keller, P., De Strooper, B., Beyreuther, K., Dotti, C. G. and Simons, K. (1998) Cholesterol depletion inhibits the generation of beta-amyloid in hippocampal neurons. *Proc. Natl. Acad. Sci. USA*, **95**, 6460–6464.
7. Refolo, L.M., Pappolla, M.A., LaFrancois, J., Malester, B., Schmidt, S.D., Thomas-Bryant, T., Tint, G.S., Wang, R., Merckken, M., Petanceska, S.S. *et al.* (2001) A cholesterol-lowering drug reduces beta-amyloid pathology in a transgenic mouse model of Alzheimer's disease. *Neurobiol. Dis.*, **8**, 890–899.
8. Fryer, J.D., Demattos, R.B., McCormick, L.M., O'Dell, M.A., Spinner, M.L., Bales, K.R., Paul, S.M., Sullivan, P.M., Parsadanian, M., Bu, G. *et al.* (2005) The low density lipoprotein receptor regulates the level of central nervous system human and murine apolipoprotein E but does not modify amyloid plaque pathology in PDAPP mice. *J. Biol. Chem.*, **280**, 25754–25759.
9. George, A.J., Holsinger, R.M., McLean, C.A., Laughton, K.M., Beyreuther, K., Evin, G., Masters, C.L. and Li, Q.X. (2004) APP intracellular domain is increased and soluble Abeta is reduced with diet-induced hypercholesterolemia in a transgenic mouse model of Alzheimer disease. *Neurobiol. Dis.*, **16**, 124–132.
10. Fagan, A.M., Christopher, E., Taylor, J.W., Parsadanian, M., Spinner, M., Watson, M., Fryer, J.D., Wahrle, S., Bales, K.R., Paul, S.M. *et al.* (2004) ApoAI deficiency results in marked

reductions in plasma cholesterol but no alterations in amyloid-beta pathology in a mouse model of Alzheimer's disease-like cerebral amyloidosis. *Am. J. Pathol.*, **165**, 1413–1422.
11. Abad-Rodriguez, J., Ledesma, M.D., Craessaerts, K., Perga, S., Medina, M., Delacourte, A., Dingwall, C., De Strooper, B. and Dotti, C.G. (2004) Neuronal membrane cholesterol loss enhances amyloid peptide generation. *J. Cell. Biol.*, **167**, 953–960.
12. Park, I.H., Hwang, E.M., Hong, H.S., Boo, J.H., Oh, S.S., Lee, J., Jung, M.W., Bang, O.Y., Kim, S.U. and Mook-Jung, I. (2003) Lovastatin enhances Abeta production and senile plaque deposition in female Tg2576 mice. *Neurobiol. Aging*, **24**, 637–643.
13. Dietschy, J.M. and Turley, S.D. (2001) Cholesterol metabolism in the brain. *Curr. Opin. Lipidol.*, **12**, 105–112.
14. Maulik, M., Westaway, D., Jhamandas, J.H. and Kar, S. (2013) Role of cholesterol in APP metabolism and its significance in Alzheimer's disease pathogenesis. *Mol. Neurobiol.*, **47**, 37–63.
15. Vance, J.E. and Karten, B. (2014) Niemann-Pick C disease and mobilization of lysosomal cholesterol by cyclodextrin. *J. Lipid. Res.*, **55**, 1609–1621.
16. Vanier, M.T. (2015) Complex lipid trafficking in Niemann-Pick disease type C. *J. Inherit. Metab. Dis.*, **38**, 187–199.
17. Peake, K.B. and Vance, J.E. (2010) Defective cholesterol trafficking in Niemann-Pick C-deficient cells. *FEBS. Lett.*, **584**, 2731–2739.
18. Karten, B., Vance, D.E., Campenot, R.B. and Vance, J.E. (2002) Cholesterol accumulates in cell bodies, but is decreased in distal axons, of Niemann-Pick C1-deficient neurons. *J. Neurochem.*, **83**, 1154–1163.
19. Nixon, R.A. (2005) Endosome function and dysfunction in Alzheimer's disease and other neurodegenerative diseases. *Neurobiol. Aging*, **26**, 373–382.
20. Jin, L.W., Shie, F.S., Maezawa, I., Vincent, I. and Bird, T. (2004) Intracellular accumulation of amyloidogenic fragments of amyloid-beta precursor protein in neurons with Niemann-Pick type C defects is associated with endosomal abnormalities. *Am. J. Pathol.*, **164**, 975–985.
21. Kagedal, K., Kim, W.S., Appelqvist, H., Chan, S., Cheng, D., Agholme, L., Barnham, K., McCann, H., Halliday, G. and Garner, B. (2010) Increased expression of the lysosomal cholesterol transporter NPC1 in Alzheimer's disease. *Biochim. Biophys. Acta*, **1801**, 831–838.
22. Malnar, M., Hecimovic, S., Mattsson, N. and Zetterberg, H. (2014) Bidirectional links between Alzheimer's disease and Niemann-Pick type C disease. *Neurobiol. Dis.*, **72**(Pt A), 37–47.
23. Mattsson, N., Zetterberg, H., Bianconi, S., Yanjanin, N.M., Fu, R., Mansson, J.E., Porter, F.D. and Blennow, K. (2011) Gamma-secretase-dependent amyloid-beta is increased in Niemann-Pick type C: a cross-sectional study. *Neurology*, **76**, 366–372.
24. Saito, Y., Suzuki, K., Nanba, E., Yamamoto, T., Ohno, K. and Murayama, S. (2002) Niemann-Pick type C disease: accelerated neurofibrillary tangle formation and amyloid beta deposition associated with apolipoprotein E epsilon 4 homozygosity. *Ann. Neurol.*, **52**, 351–355.
25. Maulik, M., Ghoshal, B., Kim, J., Wang, Y., Yang, J., Westaway, D. and Kar, S. (2012) Mutant human APP exacerbates pathology in a mouse model of NPC and its reversal by a beta-cyclodextrin. *Hum. Mol. Genet.*, **21**, 4857–4875.
26. Leem, J.Y., Saura, C.A., Pietrzik, C., Christianson, J., Wanamaker, C., King, L.T., Veselits, M.L., Tomita, T., Gasparini, L., Iwatsubo, T. *et al.* (2002) A role for presenilin 1 in regulating the delivery of amyloid precursor protein to the cell surface. *Neurobiol. Dis.*, **11**, 64–82.
27. Rebelo, S., Vieira, S.I., da Cruz, E.S.E.F. and da Cruz, E.S.O.A. (2008) Monitoring "De Novo"APP synthesis by taking advantage of the reversible effect of cycloheximide. *Am. J. Alzheimers Dis. Other Demen.*, **23**, 602–608.
28. Ihara, Y., Morishima-Kawashima, M. and Nixon, R. (2012) The ubiquitin-proteasome system and the autophagic-lysosomal system in Alzheimer disease. *Cold Spring Harb. Perspect. Med.*, **2**, doi: 10.1101/cshperspect.a006361.
29. Hong, L., Huang, H.C. and Jiang, Z.F. (2014) Relationship between amyloid-beta and the ubiquitin-proteasome system in Alzheimer's disease. *Neurol. Res.*, **36**, 276–282.
30. van Meel, E. and Klumperman, J. (2008) Imaging and imagination: understanding the endo-lysosomal system. *Histochem. Cell Biol.*, **129**, 253–266.
31. Barth, J.M. and Kohler, K. (2014) How to take autophagy and endocytosis up a notch. *Biomed. Res. Int.*, **2014**, 960803.
32. Guo, Q., Li, H., Gaddam, S.S., Justice, N.J., Robertson, C.S. and Zheng, H. (2012) Amyloid precursor protein revisited: neuron-specific expression and highly stable nature of soluble derivatives. *J. Biol. Chem.*, **287**, 2437–2445.
33. Villegas, C., Muresan, V. and Ladescu Muresan, Z. (2014) Dual-tagged amyloid-beta precursor protein reveals distinct transport pathways of its N- and C-terminal fragments. *Hum. Mol. Genet.*, **23**, 1631–1643.
34. Xilouri, M. and Stefanis, L. (2010) Autophagy in the central nervous system: implications for neurodegenerative disorders. *CNS Neurol. Disord. Drug Targets*, **9**, 701–719.
35. Ghavami, S., Shojaei, S., Yeganeh, B., Ande, S.R., Jangamreddy, J.R., Mehrpour, M., Christoffersson, J., Chaabane, W., Moghadam, A.R., Kashani, H.H. *et al.* (2014) Autophagy and apoptosis dysfunction in neurodegenerative disorders. *Prog. Neurobiol.*, **112**, 24–49.
36. Rogov, V., Dotsch, V., Johansen, T. and Kirkin, V. (2014) Interactions between autophagy receptors and ubiquitin-like proteins form the molecular basis for selective autophagy. *Mol. Cell*, **53**, 167–178.
37. Salminen, A., Kaarniranta, K., Kauppinen, A., Ojala, J., Haapasalo, A., Soininen, H. and Hiltunen, M. (2013) Impaired autophagy and APP processing in Alzheimer's disease: The potential role of Beclin 1 interactome. *Prog. Neurobiol.*, **106–107**, 33–54.
38. Nilsson, P. and Saido, T.C. (2014) Dual roles for autophagy: degradation and secretion of Alzheimer's disease Abeta peptide. *Bioessays*, **36**, 570–578.
39. Thome, R., Lopes, S.C., Costa, F.T. and Verinaud, L. (2013) Chloroquine: modes of action of an undervalued drug. *Immunol. Lett.*, **153**, 50–57.
40. Ganley, I.G., Wong, P.M., Gammoh, N. and Jiang, X. (2011) Distinct autophagosomal-lysosomal fusion mechanism revealed by thapsigargin-induced autophagy arrest. *Mol. Cell*, **42**, 731–743.
41. Blommaart, E.F., Krause, U., Schellens, J.P., Vreeling-Sindelarova, H. and Meijer, A.J. (1997) The phosphatidylinositol 3-kinase inhibitors wortmannin and LY294002 inhibit autophagy in isolated rat hepatocytes. *Eur. J. Biochem.*, **243**, 240–246.
42. Petiot, A., Ogier-Denis, E., Blommaart, E.F., Meijer, A.J. and Codogno, P. (2000) Distinct classes of phosphatidylinositol 3′-kinases are involved in signaling pathways that control macroautophagy in HT-29 cells. *J. Biol. Chem.*, **275**, 992–998.
43. Stroikin, Y., Dalen, H., Loof, S. and Terman, A. (2004) Inhibition of autophagy with 3-methyladenine results in impaired turnover of lysosomes and accumulation of lipofuscin-like material. *Eur. J. Cell. Biol.*, **83**, 583–590.
44. Yang, Y.P., Hu, L.F., Zheng, H.F., Mao, C.J., Hu, W.D., Xiong, K.P., Wang, F. and Liu, C.F. (2013) Application and interpretation of

current autophagy inhibitors and activators. *Acta Pharmacol. Sin.*, **34**, 625–635.
45. Swomley, A.M., Forster, S., Keeney, J.T., Triplett, J., Zhang, Z., Sultana, R. and Butterfield, D.A. (2014) Abeta, oxidative stress in Alzheimer disease: evidence based on proteomics studies. *Biochim. Biophys. Acta*, **1842**, 1248–1257.
46. Vazquez, M.C., Balboa, E., Alvarez, A.R. and Zanlungo, S. (2012) Oxidative stress: a pathogenic mechanism for Niemann-Pick type C disease. *Oxid. Med. Cell Longev.*, **2012**, 205713.
47. Berger-Sweeney, J., McPhie, D.L., Arters, J.A., Greenan, J., Oster-Granite, M.L. and Neve, R.L. (1999) Impairments in learning and memory accompanied by neurodegeneration in mice transgenic for the carboxyl-terminus of the amyloid precursor protein. *Brain Res. Mol. Brain Res.*, **66**, 150–162.
48. Bignante, E.A., Heredia, F., Morfini, G. and Lorenzo, A. (2013) Amyloid beta precursor protein as a molecular target for amyloid beta-induced neuronal degeneration in Alzheimer's disease. *Neurobiol. Aging*, **34**, 2525–2537.
49. Wirths, O., Multhaup, G. and Bayer, T.A. (2004) A modified beta-amyloid hypothesis: intraneuronal accumulation of the beta-amyloid peptide—the first step of a fatal cascade. *J. Neurochem.*, **91**, 513–520.
50. Bove, J., Martinez-Vicente, M. and Vila, M. (2011) Fighting neurodegeneration with rapamycin: mechanistic insights. *Nat. Rev. Neurosci.*, **12**, 437–452.
51. Shen, H.M. and Mizushima, N. (2014) At the end of the autophagic road: an emerging understanding of lysosomal functions in autophagy. *Trends Biochem. Sci.*, **39**, 61–71.
52. Puglielli, L., Tanzi, R.E. and Kovacs, D.M. (2003) Alzheimer's disease: the cholesterol connection. *Nat. Neurosci.*, **6**, 345–351.
53. Burgess, B.L., Parkinson, P.F., Racke, M.M., Hirsch-Reinshagen, V., Fan, J., Wong, C., Stukas, S., Theroux, L., Chan, J.Y., Donkin, J. *et al.* (2008) ABCG1 influences the brain cholesterol biosynthetic pathway but does not affect amyloid precursor protein or apolipoprotein E metabolism in vivo. *J. Lipid Res.*, **49**, 1254–1267.
54. Halford, R.W. and Russell, D.W. (2009) Reduction of cholesterol synthesis in the mouse brain does not affect amyloid formation in Alzheimer's disease, but does extend lifespan. *Proc. Natl. Acad. Sci. U.S.A.*, **106**, 3502–3506.
55. Kodam, A., Maulik, M., Peake, K., Amritraj, A., Vetrivel, K.S., Thinakaran, G., Vance, J.E. and Kar, S. (2010) Altered levels and distribution of amyloid precursor protein and its processing enzymes in Niemann-Pick type C1-deficient mouse brains. *Glia*, **58**, 1267–1281.
56. Burns, M., Gaynor, K., Olm, V., Mercken, M., LaFrancois, J., Wang, L., Mathews, P.M., Noble, W., Matsuoka, Y. and Duff, K. (2003) Presenilin redistribution associated with aberrant cholesterol transport enhances beta-amyloid production in vivo. *J. Neurosci.*, **23**, 5645–5649.
57. Yamazaki, T., Chang, T.Y., Haass, C. and Ihara, Y. (2001) Accumulation and aggregation of amyloid beta-protein in late endosomes of Niemann-pick type C cells. *J. Biol. Chem.*, **276**, 4454–4460.
58. Fraser, P.E., Levesque, G., Yu, G., Mills, L.R., Thirlwell, J., Frantseva, M., Gandy, S.E., Seeger, M., Carlen, P.L. and St George-Hyslop, P. (1998) Presenilin 1 is actively degraded by the 26S proteasome. *Neurobiol. Aging*, **19**, S19–S21.
59. He, G., Qing, H., Tong, Y., Cai, F., Ishiura, S. and Song, W. (2007) Degradation of nicastrin involves both proteasome and lysosome. *J. Neurochem.*, **101**, 982–992.
60. Qing, H., Zhou, W., Christensen, M.A., Sun, X., Tong, Y. and Song, W. (2004) Degradation of BACE by the ubiquitin-proteasome pathway. *FASEB J.*, **18**, 1571–1573.
61. Aboukhatwa, M. and Luo, Y. (2011) Antidepressants modulate intracellular amyloid peptide species in N2a neuroblastoma cells. *J. Alzheimers Dis.*, **24**, 221–234.
62. Cho, S.J., Yun, S.M., Jo, C., Lee, D.H., Choi, K.J., Song, J.C., Park, S.I., Kim, Y.J. and Koh, Y.H. (2015) SUMO1 promotes Abeta production via the modulation of autophagy. *Autophagy*, **11**, 100–112.
63. Majd, S., Chegini, F., Chataway, T., Zhou, X.F. and Gai, W. (2013) Reciprocal induction between alpha-synuclein and beta-amyloid in adult rat neurons. *Neurotox. Res.*, **23**, 69–78.
64. Yu, W.H., Cuervo, A.M., Kumar, A., Peterhoff, C.M., Schmidt, S. D., Lee, J.H., Mohan, P.S., Mercken, M., Farmery, M.R., Tjernberg, L.O. *et al.* (2005) Macroautophagy—a novel beta-amyloid peptide-generating pathway activated in Alzheimer's disease. *J. Cell. Biol.*, **171**, 87–98.
65. Zheng, L., Terman, A., Hallbeck, M., Dehvari, N., Cowburn, R. F., Benedikz, E., Kagedal, K., Cedazo-Minguez, A. and Marcusson, J. (2011) Macroautophagy-generated increase of lysosomal amyloid beta-protein mediates oxidant-induced apoptosis of cultured neuroblastoma cells. *Autophagy*, **7**, 1528–1545.
66. Jaeger, P.A., Pickford, F., Sun, C.H., Lucin, K.M., Masliah, E. and Wyss-Coray, T. (2010) Regulation of amyloid precursor protein processing by the Beclin 1 complex. *PLoS One*, **5**, e11102.
67. Hung, S.Y., Huang, W.P., Liou, H.C. and Fu, W.M. (2009) Autophagy protects neuron from Abeta-induced cytotoxicity. *Autophagy*, **5**, 502–510.
68. Tian, Y., Bustos, V., Flajolet, M. and Greengard, P. (2011) A small-molecule enhancer of autophagy decreases levels of Abeta and APP-CTF via Atg5-dependent autophagy pathway. *FASEB J.*, **25**, 1934–1942.
69. Boland, B., Smith, D.A., Mooney, D., Jung, S.S., Walsh, D.M. and Platt, F.M. (2010) Macroautophagy is not directly involved in the metabolism of amyloid precursor protein. *J. Biol. Chem.*, **285**, 37415–37426.
70. Kaufmann, A.M., Goldman, S.D. and Krise, J.P. (2009) A fluorescence resonance energy transfer-based approach for investigating late endosome-lysosome retrograde fusion events. *Anal. Biochem.*, **386**, 91–97.
71. Goldman, S.D. and Krise, J.P. (2010) Niemann-Pick C1 functions independently of Niemann-Pick C2 in the initial stage of retrograde transport of membrane-impermeable lysosomal cargo. *J. Biol. Chem.*, **285**, 4983–4994.
72. Koh, C.H., Whiteman, M., Li, Q.X., Halliwell, B., Jenner, A.M., Wong, B.S., Laughton, K.M., Wenk, M., Masters, C.L., Beart, P.M. *et al.* (2006) Chronic exposure to U18666A is associated with oxidative stress in cultured murine cortical neurons. *J. Neurochem.*, **98**, 1278–1289.
73. Lloyd-Evans, E., Morgan, A.J., He, X., Smith, D.A., Elliot-Smith, E., Sillence, D.J., Churchill, G.C., Schuchman, E.H., Galione, A. and Platt, F.M. (2008) Niemann-Pick disease type C1 is a sphingosine storage disease that causes deregulation of lysosomal calcium. *Nat. Med.*, **14**, 1247–1255.
74. Zampieri, S., Mellon, S.H., Butters, T.D., Nevyjel, M., Covey, D.F., Bembi, B. and Dardis, A. (2009) Oxidative stress in NPC1 deficient cells: protective effect of allopregnanolone. *J. Cell Mol. Med.*, **13**, 3786–3796.
75. Blurton-Jones, M. and Laferla, F.M. (2006) Pathways by which Abeta facilitates tau pathology. *Curr. Alzheimer Res.*, **3**, 437–448.
76. Stancu, I.C., Vasconcelos, B., Terwel, D. and Dewachter, I. (2014) Models of beta-amyloid induced Tau-pathology: the long and "folded" road to understand the mechanism. *Mol. Neurodegener.*, **9**, 51.

77. Meda, L., Baron, P. and Scarlato, G. (2001) Glial activation in Alzheimer's disease: the role of Abeta and its associated proteins. *Neurobiol. Aging*, **22**, 885–893.
78. von Bernhardi, R. (2007) Glial cell dysregulation: a new perspective on Alzheimer disease. *Neurotox. Res.*, **12**, 215–232.
79. Chishti, M.A., Yang, D.S., Janus, C., Phinney, A.L., Horne, P., Pearson, J., Strome, R., Zuker, N., Loukides, J., French, J. *et al.* (2001) Early-onset amyloid deposition and cognitive deficits in transgenic mice expressing a double mutant form of amyloid precursor protein 695. *J. Biol. Chem.*, **276**, 21562–21570.
80. Thinakaran, G., Teplow, D.B., Siman, R., Greenberg, B. and Sisodia, S.S. (1996) Metabolism of the "Swedish" amyloid precursor protein variant in neuro2a (N2a) cells. Evidence that cleavage at the "beta-secretase" site occurs in the Golgi apparatus. *J. Biol. Chem.*, **271**, 9390–9397.
81. Grimm, M.O., Grimm, H.S., Tomic, I., Beyreuther, K., Hartmann, T. and Bergmann, C. (2008) Independent inhibition of Alzheimer disease beta- and gamma-secretase cleavage by lowered cholesterol levels. *J. Biol. Chem.*, **283**, 11302–11311.
82. Mathur, B.N., Neely, M.D., Dyllick-Brenzinger, M., Tandon, A. and Deutch, A.Y. (2007) Systemic administration of a proteasome inhibitor does not cause nigrostriatal dopamine degeneration. *Brain Res.*, **1168**, 83–89.
83. Song, M.S., Rauw, G., Baker, G.B. and Kar, S. (2008) Memantine protects rat cortical cultured neurons against beta-amyloid-induced toxicity by attenuating tau phosphorylation. *Eur. J. Neurosci.*, **28**, 1989–2002.